

ADA055789

AFFDL-TR-77-58

A STUDY OF ANALOG PROGRAMMING FOR PREDICTION
OF CRACK GROWTH IN AIRCRAFT STRUCTURES
SUBJECTED TO RANDOM LOADS

Aeroelastic and Structures Research Laboratory
Department of Aeronautics and Astronautics
Massachusetts Institute of Technology
Cambridge, Massachusetts 02139

June 1977

Technical Report AFFDL-TR-77-58
Final Report for Period September 1976 - June 1977

Approved for public release; distribution unlimited

AIR FORCE FLIGHT DYNAMICS LABORATORY
AIR FORCE WRIGHT AERONAUTICAL LABORATORIES
AIR FORCE SYSTEMS COMMAND
WRIGHT-PATTERSON AIR FORCE BASE, OHIO 45433

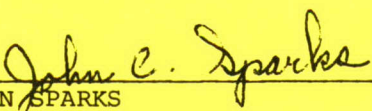
20080820 012

NOTICE

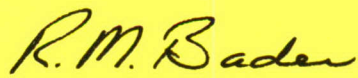
When Government drawings, specifications, or other data are used for any purpose other than in connection with a definitely related Government procurement operation, the United States Government thereby incurs no responsibility nor any obligation whatsoever; and the fact that the Government may have formulated, furnished, or in any way supplied the said drawings, specifications, or other data, is not to be regarded by implication or otherwise as in any manner licensing the holder or any other person or corporation, or conveying any rights or permission to manufacturer, use, or sell any patented invention that may in any way be related thereto.

This report has been reviewed by the Information Office (OI) and is releasable to the National Technical Information Service (NTIS). At NTIS, it will be available to the general public, including foreign nations.

This technical report has been reviewed and is approved for publication.

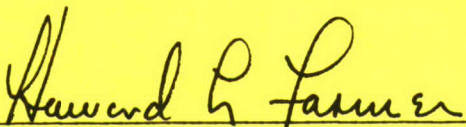


JOHN SPARKS
Project Engineer



ROBERT M. BADER, Chief
Structural Integrity Branch
Structures Division

FOR THE COMMANDER



HOWARD L. FARMER, Colonel, USAF
Chief, Structural Mechanics Division

Copies of this report should not be returned unless return is required by security considerations, contractual obligations, or notice on a specific document.

REPORT DOCUMENTATION PAGE		READ INSTRUCTIONS BEFORE COMPLETING FORM
1. REPORT NUMBER AFFDL-TR-77-58	2. GOVT ACCESSION NO. NA	3. RECIPIENT'S CATALOG NUMBER NA
4. TITLE (and Subtitle) A STUDY OF ANALOG PROGRAMMING FOR PREDICTION OF CRACK GROWTH IN AIRCRAFT STRUCTURES SUBJECTED TO RANDOM LOADS		5. TYPE OF REPORT & PERIOD COVERED FINAL Sept. 1976 - June 1977
		6. PERFORMING ORG. REPORT NUMBER ASRL TR 186-2
7. AUTHOR(s) Michael Weinreich John F. McCarthy, Jr. Richard F. Harris Oscar Orringer		8. CONTRACT OR GRANT NUMBER(s) F33615-76-C-3109
9. PERFORMING ORGANIZATION NAME AND ADDRESS Aeroelastic and Structures Research Laboratory Massachusetts Institute of Technology Cambridge, MA 02139		10. PROGRAM ELEMENT, PROJECT, TASK AREA & WORK UNIT NUMBERS Project No. 1367 Task No. 136703 Work Unit 13670330
11. CONTROLLING OFFICE NAME AND ADDRESS Air Force Flight Dynamics Laboratory Attn: AFFDL/FBE Wright-Patterson Air Force Base, Ohio 45433		12. REPORT DATE June 1977
		13. NUMBER OF PAGES 85
14. MONITORING AGENCY NAME & ADDRESS (if different from Controlling Office) Same		15. SECURITY CLASS. (of this report) Unclassified
		15a. DECLASSIFICATION/DOWNGRADING SCHEDULE
16. DISTRIBUTION STATEMENT (of this Report) Approved for public release; distribution unlimited		
17. DISTRIBUTION STATEMENT (of the abstract entered in Block 20, if different from Report) Same		
18. SUPPLEMENTARY NOTES None		
19. KEY WORDS (Continue on reverse side if necessary and identify by block number) Crack Propagation Monte Carlo Simulation Risk Analysis Estimation Theory Analog Computers		
20. ABSTRACT (Continue on reverse side if necessary and identify by block number) Results of a program to study an analog approach to risk analysis of random-load crack growth are presented. The two major objectives were to implement certain specific simulations of crack growth on hybrid analog/digital hardware, and to develop an improved approach to the modeling of random loads. Under the first objective, all but two of the specific simulations were implemented and verified. One not implemented required hardware unavailable at the installation utilized for the simulations. The other was identified as not conducive to analog simulation. These simulations utilized a "damage parameter" (rather		

than crack size itself as the random variable) to provide well behaved and stable analog behavior.

Under the second objective, a method of generating load statistics by direct inspection of large quantities of flight data was developed. In the course of this development, the applicability of estimation theory to the present problem was identified. The techniques of estimation theory, applied to analysis of damage in terms of an appropriately chosen damage parameter, promise to provide improved efficiency and accuracy in aircraft fatigue damage risk analysis.

The program has resulted in three major recommendations concerning aircraft fatigue damage risk analysis. First, the use of a suitably defined "damage parameter", rather than crack size itself, is recommended for any statistical analysis of fatigue damage regardless of the approach taken. Second, direct inspection of large quantities of flight data is recommended to obtain the important statistics of loading sequences for utilization in any risk analysis. Third, further development of the application of estimation theory to aircraft fatigue damage risk analysis is recommended.

ADA055789

FOREWORD

The developments documented in this report were carried out at the Aeroelastic and Structures Research Laboratory, Massachusetts Institute of Technology, Cambridge, Massachusetts 02139, under Contract No. F33615-76-C-3109 (Project 1367, Task 136703) from the U.S. Air Force Flight Dynamics Laboratory. Mr. John Sparks (AFFDL/FBE) served as technical monitor. The analog programs discussed in Section III were implemented and verified under subcontract by the Colorado Institute of Structural Mechanics, Littleton, Colorado 80122. The authors wish to express their appreciation to Captain John Mazzae (ASD/ADSD) for his advice and generous assistance in implementing the analog programs at the USAF Aeronautical Systems Division Scientific Computing Facility.

TABLE OF CONTENTS

<u>Section</u>		<u>Page</u>
I	INTRODUCTION	1
	1.1 Program Objectives	1
	1.2 Modeling the Physical Problem	2
	1.3 Results of Previous and Present Programs	4
II	FORMULATION FOR COMPUTATION OF CRACK-GROWTH STATISTICS	7
	2.1 The Damage Parameter "h"	7
	2.2 The Statistics of Random Loading	12
	2.3 Derivation of Crack-Size Statistics	18
	2.4 Reanalysis of Previous Monte Carlo Simulation	21
	2.5 Utilization of Density Moments	24
III	ANALOG SIMULATION OF CRACK GROWTH	27
	3.1 Results for Specific Tasks	27
	3.1.1 Forman Equation	27
	3.1.2 Retardation	28
	3.1.3 Local Geometry Effects	30
	3.1.4 Randomized GAG Sequence	32
	3.1.5 Superposition of Random Flight Loads and GAG Cycles	34
	3.1.6 Random Initial Condition	35
	3.1.7 Simulation of Random Maneuver Loads	36
	3.1.8 Incorporation of Threshold Effect	37
	3.1.9 Coupled Dynamics for Two Cracks	38
	3.2 Evaluation of Results	39
	3.3 Equipment Availability	41
IV	CONCLUSIONS AND RECOMMENDATIONS	43
	4.1 Summary	43
	4.2 Estimation Theory for the Prediction of Crack-Growth Statistics	44
	4.3 Discussion and Conclusions	49
	4.4 Recommendations	50

TABLE OF CONTENTS
(concluded)

<u>Section</u>	<u>Page</u>
APPENDICES	
A FORTRAN Program for Calculation of Crack-Growth Statistics	75
B Sample Output	79
C Commercial Hybrid Computer Manufacturers	81
D Hybrid Computer Features	82
REFERENCES	83

LIST OF ILLUSTRATIONS

<u>Figure</u>		<u>Page</u>
1	Comparison of Time-Histories of Crack Size and Damage Parameter for Paris Equation	52
2	Comparison of Time-Histories of Crack Size and Damage Parameter for Forman Equation	53
3	Comparison of Time-Histories of Damage Parameter for Paris Equation, for $N_p > 2$ and $N_p < 2$	54
4	Comparison of Time Histories of Damage Parameter $h = \ln(a)$ for Paris Equation with N_p Near Two	55
5	Probability Density Functions for s_{\max} and Δs , for Band-Limited White Noise	56
6	Reduction of Sampled Flight Data to Load Statistics	57
7	Examination of Sample-and-Hold Circuitry	58
8	Forman Equation Flow Chart, Using Damage Parameter "h"	59
9	Analog Simulation of Forman Equation (Real Time)	60
10	Analog Simulation of Forman Equation (Repetitive Operation)	61
11	Finite Plate Correlation Factor for Plate Width $b=10$ Inches	62
12	Analog Diagram for Random Appearance of a Deterministic GAG Cycle	62
13	Effect of Switching Voltage Bias on Average Time Between GAG Cycles	63
14	Analog Diagram for GAG/Flight Load Superposition	64
15	Simulation of Hypothetical Flight with Three Segments	65
16	Gain Function for Weibull Distribution Shaping	66
17	Shaping Filter for Rayleigh Noise	67
18	Stress Intensity Threshold Flow Chart	68
19	Analog Simulation of Forman Equation with Stress Intensity Threshold	69
20	Flow Chart for Simulation of Coupled Crack Growth	70
21	Analog Simulation of the Growth of Two Coupled Cracks with Different Initial Sizes	71

LIST OF ILLUSTRATIONS
(concluded)

<u>Figure</u>		<u>Page</u>
22	Analog Simulation of the Growth of Two Initially Equal Coupled Cracks at Different Rates	72
23	Schematic Diagram of Estimation Theory	73
24	Treatment of Bimodal Crack Population	74

Section I

INTRODUCTION

1.1 Program Objectives

The Air Force Aircraft Structural Integrity Program (ASIP) includes requirements for fracture mechanics analyses of aircraft fleets to assess safety limits and establish inspection intervals. This portion of the ASIP includes requirements for calculation of the size (as a function of flight time) of cracks which might be present in fleet airframes [1]. The initial conditions for the calculations are cracks of prescribed size and shape (specific to various structural details). The size and shape values are based in part upon observations of actual airframe cracks from past service experience, and in part upon the degree of inspectability of the airframe [2]. The crack-growth calculations, as currently required, seek to assess crack size versus time for the deterministic initial conditions outlined above and for load time-histories also assumed to be deterministic. The load spectra are prepared by assembly of detailed profiles for each segment (taxi, climb, cruise, etc.) of each mission type (cargo haul, training, air/air combat, etc.) which the fleet is expected to fly [3].

In reality, variability appears in the actual initial-crack sizes, in the load spectra (through individual aircraft usage variation), in material properties, and in manufacturing details. Fleet airframes may therefore contain a population of cracks with sizes governed by a time-dependent probability distribution. The ASIP criteria seek to assess the effect of average loads on the growth of above-average initial cracks. Risk analysis is an associated structural integrity assessment function which in some cases seeks to quantify the abnormal possibilities (extremely large initial crack size, above-average loads) in terms of a probability model. Risk analyses of the latter type require a tremendous volume of repetitive calculations. The objectives of this program were to assess the capabilities of hybrid analog/digital computers to perform such analyses in an efficient manner, and to employ random-process theory to obtain an improved description of the random components of loading for use in risk analysis.

The first program objective was organized as ten specific tasks, nine involving the implementation, verification and evaluation of an analog simulation of one or more aspects of currently accepted crack growth-rate models. The

evaluation included an assessment of the ability of currently available Air Force analog computing facilities to accommodate the simulations. The second program objective was to develop a compatible analog-based method for simulating two-parameter load models (i.e. stress peaks and ranges, mean and alternating stresses, or stress ranges and ratios) based on power spectra and/or peak-exceedance curves representative of an aircraft load history.

1.2 Modeling the Physical Problem

Formulation of a mathematical model of the physical problem of crack growth under random initial conditions and random loading is a difficult and extremely important step. Every effort must be made to insure that the mathematical model adequately represents the physical situation, but is not so complicated as to preclude numerical calculations because of excessive costs. Also, the model must utilize a data base which is very large, but not very complete. The procedures used to develop the model are summarized in the following paragraphs.

The mathematical model can be separated into two parts. The first part is the environment encountered by the structure, viz: the random and non-random components of loading. The second part is the crack-propagation behavior which results from the loading.

When developing the loading model, every effort is made to maintain accuracy for those statistics which are important in crack propagation, while economies are instituted for those statistics which have less effect on crack growth-rates. Numerous investigators in the past have treated aircraft loading as a Gaussian random process. In a recent investigation, Shinozuka [4] considered flight-by-flight loading to consist of ground loads, gust loads, GAG cycles, and maneuver loads, for which:

"[The experimental evidence] tends to indicate that most of the gust loading and the maneuver loading for cargo or transport type airplanes can be modeled by composite Gaussian processes while the maneuver loading for fighter type airplanes can be approximated more closely by single Gaussian processes."

However, other evidence, such as studies of air turbulence models for use in flight simulators [5] and estimates of fighter peak- n_z -exceedance curves based in part on flight data and in part on V_{gh} calculations [6] provide some evidence of non-Gaussian characteristics of loading.

Crack-propagation behavior has been shown to depend primarily upon the sequence of stress minima and maxima occurring at critical locations in the structure, coupled with the instantaneous size of the fatigue crack. The rate of crack growth depends primarily on the difference, Δs , between each minimum and its succeeding maximum. The Paris equation, the simplest form of crack-propagation model, shows dependence only on this difference [7]. This is essentially a linear damage-summation model similar to the Palmgren-Miner hypothesis [8,9]. Linear damage-summation models possess an appealing simplicity especially convenient for applications to random loading, in that the sum of crack-size increments for many load cycles is independent of the specific load sequence. Hence, the statistics of the crack-increment sum can be related directly to the time-average statistics of a random process which describes the loading. Forman et al. [10] have included a "layering" effect depending on the ratio of successive values of stress minima and maxima, and an "acceleration" effect depending on the ratio of the applied crack-tip stress intensity factor to the material fracture toughness, providing a greatly improved model. With only the "layering" effect, this is still essentially a linear damage-summation model. With the incorporation of the "acceleration" effect, the time-average statistics of the random loading are no longer sufficient, so if those statistics are nonstationary, then such nonstationary statistics must be provided. With this required statistical description of the loading, most of the appealing simplicity of the linear damage-summation models remains. Simplified random-process models for damage accumulation have been developed based on Miner's rule [11] and on the Forman equation for crack-propagation [12].

However, the work of Schjive [13] and others has shown that fatigue crack-ing in structures is in many cases sensitive to the specific load-application sequence. This effect derives from the material "memory" associated with plastic yielding and subsequent residual stresses near the crack tip. Modifications of the linear damage-summation models for crack-propagation have been made by Wheeler [14], Willenborg et al [15], Dill and Saff [16], and others to account for material memory effects. Past implementations of these models have generally required cycle-by-cycle summation of crack-size increments. Several efficient digital computer codes (e.g., Ref. 17) have been developed for this purpose. More recently, Gallagher [18] has shown for transport aircraft that flight-by-flight summation can be used to predict crack growth accurately if the rate

equation is formulated on a per-flight basis, with parameters fit to flight-by-flight crack-propagation test data.

With regard to load models, it was the judgment of the present investigators that load models should not be restricted to Gaussian load spectra unless both adequate modeling accuracy and simplification of the resulting analysis could be assured. As will be described in Subsection 2.2, such assurance is lacking. On the other hand, the crack-propagation models described above have been repeatedly verified by comparison of predictions with laboratory experiments using deterministic loading. Hence, the present investigators accepted these crack-propagation models in this program.

1.3 Results of Previous and Present Programs

The statistics of crack size were investigated by Monte Carlo simulation, using a small analog computer, in a previous program under Air Force Contract F33615-74-C-3046. Repeated runs with the loading simulated by a white-noise generator filtered through analog sample-and-hold circuitry yielded crack-size histograms to which 3-parameter Weibull distributions were fit by maximum-likelihood estimation [19]. Crude models were used for both the crack growth-rate behavior and the random loading because the primary objective of the investigation was to assess the feasibility of performing Monte Carlo simulation on an analog computer with the rising exponential type of dynamics generally exhibited by crack size versus time. A simplified form of the Paris equation without local geometry effects was taken as the growth-rate model:

$$da/dN \approx C_p (\Delta S \sqrt{a})^{N_p} \quad (1)$$

where

a = Instantaneous crack size

N = Number of applied stress cycles

$\Delta S = s_{\max} - s_{\min}$ = Stress range

and where C_p , N_p are empirical constants. For the purpose of the simulation, N_p was assumed equal to 4 (representative of a wide range of aluminum alloys) and C_p was fit to experimental data for a 7075-T6 alloy [20]. The stress range, Δs , was assumed as a Gaussian random process with parameters fit approximately to available fighter exceedance data [6]. The investigation did demonstrate

the feasibility of analog Monte Carlo simulation for cracks grown by random loading. However, the specific results obtained were later found to be in error due to an unexpected low-frequency resonance in the sample-and-hold circuitry which was discovered in the course of the present program.

In the present investigation, eight of nine specific simulation tasks were developed as analog programs which were implemented on a CI-5000 hybrid analog/digital computer at the USAF Aeronautical Systems Division (ASD/ADSD). Each task was demonstrated by means of a few verification runs. However, full Monte Carlo simulations were not performed for reasons which arose from developments under the remaining task in the investigation.

Development of this latter task (two-parameter simulation of random loads) led to the discovery of the low-frequency sample-and-hold resonance mentioned above. The use of sample-and-hold circuits was therefore rejected. Also, considerations of the limits of analog equipment for processing high-frequency signals led to the conclusion that much more computation time would be required for one airplane life than had previously been estimated. Hence, the analog Monte Carlo simulation approach to risk analysis appeared to be much less efficient than previously expected.

In the meantime, other developments under the load modeling task led to two ideas for improvement of the simulations. First, the crack growth-rate equations were reformulated in terms of a damage parameter which varies inversely with crack size. This transforms the dynamics of crack growth from exponential to nearly linear behavior. The new formulation was used to implement the eight specific analog simulation tasks.

Second, a general study of possible approaches to the simulation of random loads led to the concept of applying estimation theory to the crack-growth prediction problem. Estimation theory was developed by modern theorists in the field of guidance and control, primarily as a tool for optimizing designs for electronic control systems [21,22]. The present study has indicated that estimation theory can be applied to the crack-growth prediction problem to obtain the sought-after computational efficiency for risk analysis. Hence, the application of estimation theory to crack-growth dynamics was considered as a part of the random-load simulation task.

Details of the developments made under this program are presented in the following sections. Section II discusses the transformation from crack size to

damage parameter, and the benefits obtained by using a damage-parameter formulation for risk analysis of random loads and crack sizes. In Section III, the implementations of the specific analog simulation tasks are presented, together with example runs and evaluations. Section IV presents conclusions and recommendations, including discussion of the application of estimation theory to the crack-growth prediction problem.

Section II

FORMULATION FOR COMPUTATION OF CRACK-GROWTH STATISTICS

2.1 The Damage Parameter "h"

For analysis of statistics of the crack size resulting from the application of random loading to a fatigue crack, it can be very advantageous to use a damage parameter "h" in place of the crack size "a". For some mathematical models of crack propagation behavior, such as the Paris equation with no geometry factor, an appropriately chosen definition of "h" can simplify the statistical derivation to triviality. For other more complicated models, the statistical derivation is at least somewhat simplified.

The simplest commonly used model of crack propagation behavior is the Paris equation (see Eq. 1). If the growth-rate exponent N_p is chosen equal to 4 (representative of aluminum alloys), then:

$$da/dN \approx C_p (\Delta S)^4 a^2 \quad (2)$$

If the damage parameter is simply chosen as

$$h = 1/a \quad (3)$$

then substitution of Eq. 3 into Eq. 2 gives:

$$dh/dN \approx -C_p (\Delta S)^4 \quad (4)$$

The change in h then depends only on the applied loading, and not on the value of h itself. For the more general case of $N_p > 2$, the damage parameter can be chosen as

$$h = a^{1-N_p/2} \quad (5)$$

which provides

$$\frac{dh}{dN} \approx \left(1 - \frac{N_p}{2}\right) C_p (\Delta S)^{N_p} \quad (6)$$

Cases with $N_p \leq 2$ are considered later in this subsection.

Figure 1 shows constant-stress-amplitude time-histories of crack size "a" and damage parameter "h", for crack growth according to the Paris model. These histories show some problems which will affect analog simulation using crack size. Simulation of crack size will always saturate the analog equipment short of complete structural failure, as shown at (A). Scaling crack size to have its critical value a_{cr} below saturation level (B) makes the initial size quite small (C), and hence subject to analog error. This error is important because da/dN is small initially, so that a very small error in the voltage representing initial-crack size will yield a very large error in estimated time to the critical condition. This time-history is also subject to analog error at later times, because of the extreme rate of change da/dN , but this form of error will have much less effect on the estimate of time to the critical condition.

For the simple Paris model, an appropriate definition of the damage parameter "h" has eliminated the dependence of the rate of damage accumulation on the instantaneous value of accumulated damage. However, the advantages of the use of a damage parameter are reduced for more complicated and more realistic models of crack growth behavior, such as the Forman equation.

The Forman equation [10] is usually written as:

$$\frac{da}{dN} = \frac{C_F (\Delta K)^{N_F}}{(1-R)K_C - \Delta K} \quad (7)$$

where

$$\Delta K \approx \Delta S \sqrt{a} \quad (8)$$

if local geometry effects are neglected. The parameters C_F , N_F , and K_C are material constants. The crack size, a , and the stress difference $\Delta S = s_{max} - s_{min}$, are the same as for the Paris equation. The stress ratio $R = s_{min}/s_{max}$ introduces the effect of the individual values s_{min} and s_{max} .

It is convenient to substitute for ΔK , and to use ΔS and s_{max} as the descriptors of the stress. This provides the following equivalent form of the Forman equation:

$$\frac{da}{dN} \approx \frac{C_F}{K_C} (\Delta S)^{N_F} a^{N_F/2} \left[\frac{s_{max}}{\Delta S} \right] \left[\frac{s_c}{s_c - s_{max}} \right] \quad (9)$$

where

$$S_c = K_c / \sqrt{a} \quad (10)$$

Equation 9 may be considered in three parts. The first is the basic relation

$$\frac{da}{dN} \approx \frac{C_F}{K_c} (\Delta S \sqrt{a})^{N_F} \quad (11)$$

which is like the Paris equation. The second and third parts are multiplicative corrections for experimentally observed effects: the "layering" effect ($s_{\max}/\Delta s$), and the "acceleration" effect [$S_c/(S_c - s_{\max})$].

A damage parameter may be defined for the Forman equation in the same manner as was done for the Paris equation. Assuming $N_F > 2$,

$$h = a^{1-N_F/2} \quad (12)$$

$$\frac{dh}{dN} = \left(1 - \frac{N_F}{2}\right) \frac{C_F}{K_c} (\Delta S)^{N_F} \left[\frac{s_{\max}}{\Delta S}\right] \left[\frac{S_c}{S_c - s_{\max}}\right] \quad (13)$$

where

$$S_c = K_c h^{1/(N_F-2)} \quad (14)$$

This particular definition of the damage parameter results in a great simplification of the crack growth relationship, but fails to achieve the triviality found for the Paris model. The acceleration effect [$S_c/(S_c - s_{\max})$] still depends on the instantaneous value of the damage parameter. However, this dependence is fairly simple and well-behaved. Analysis of the statistics of final crack size should still be manageable.

Figure 2 shows constant-stress-amplitude time-histories of crack size "a" and damage parameter "h", for crack growth according to the Forman model. The time-history of crack size possesses the same problems as for the Paris model. The time history of the damage parameter exhibits one problem not seen with the

Paris model: large rate dh/dN near complete failure. However, this problem is not very important; it compares with the least of the problems cited for crack-size history, and is less severe. It should also be noted that if h_{cr} is based on an isolated high overload, the rate dh/dN will not increase excessively until well after h_{cr} is exceeded. This is because h_{cr} so chosen provides almost zero probability of exceedence of S_c (catastrophic structural failure) for $h > h_{cr}$ (aircraft still in service). As a result, there will be small probability of s_{max} near S_c , and consequently the crack-growth acceleration will not be severe.

Although the above choice of the damage parameter is extremely useful, a definition of a damage parameter which would eliminate all dependence of crack growth-rate on current damage would be especially desirable. Unfortunately, incorporation of the acceleration effect, which includes the value of crack size in a very different fashion from the first two effects, makes this impossible. However, there may be some methods of further simplifying the statistical analysis by changing the format of the crack-growth model. It is not necessary to use the Forman model, if another relationship can be found which provides similar agreement with the experimental data. For example, acceleration need not be modeled as a multiplicative effect. It may be additive, in which case the crack growth rate may be modeled as:

$$\frac{da}{dN} \approx \frac{C_F}{K_c} (\Delta S \sqrt{a})^{N_F} \left[\frac{S_{max}}{\Delta S} \right] + k_F \left[\frac{S_c}{S_c - S_{max}} \right] \quad (15)$$

If the same damage parameter "h" as described for the Forman equation is used, the results are the same except that the term depending on the current damage is additive rather than multiplicative. Such a change would further simplify the statistical analysis of final crack size. The use of Eq. 15 has not been pursued in this study because additive acceleration models have not been verified by comparison with experimental results.

The definitions of the damage parameter "h" presented earlier in this subsection depended on values of N_p or N_F greater than two. For some materials, such as steel, these values may be equal to or less than two, requiring different definitions of h. These definitions will be considered here using the Paris equation, and may be easily extended for application to the Forman equation.

When N_p is less than two, the mathematical definition of the damage parameter is identical to that for N_p greater than two (Eq. 5). However, the behavior of the damage parameter will be different, in that it will increase rather than decrease from its initial value, as shown in Fig. 3. When $N_p < 2$, "h" will reach infinity when crack size "a" reaches infinity, so it is clear that for the ideal case of a semi-infinite plate complete structural failure will not occur in finite time. This compares with the earlier case of $N_p > 2$, where "h" reached zero when "a" reached infinity, and complete structural failure did occur in finite time for the ideal case.

When N_p is equal to 2, Eq. 5 is singular, and an entirely new definition must be found. If the damage parameter is defined as

$$h = \ln(a) \quad (16)$$

then the Paris equation becomes

$$\frac{dh}{dN} = C_p (\Delta S)^2 \quad (17)$$

As in the case of $N_p < 2$, h increases with time, and an infinite value of h represents complete structural failure.

No matter what the value of N_p , it is not necessary to utilize the definition of "h" which reduces the Paris equation to an exactly constant rate of change of "h". Such a definition, as presented for various values of N_p so far in this subsection will be referred to as the "natural" definition and is desirable in that it simplifies the ensuing analysis. However, if the definition of the damage parameter is chosen for a value of N_p different from but close to the actual value, the analysis will remain sufficiently simple. For the case of the Forman equation, where the rate of change of h is not exactly constant even for the natural definition of h, there may be no noticeable increase in analytical difficulty. In fact, the analysis with the Forman equation may even be simplified by defining the damage parameter so that the time rate of change of h is as constant as possible including consideration of the layering and acceleration effects. This is accomplished by defining h as if N_p were somewhat larger than its actual value. It cannot be over-emphasized that the definition of h utilized for a particular analysis is a

free choice by the analyst, and its relation to the natural definition of h for the particular crack growth rate equation is guided only by the analyst's desire to obtain a simple and accurate analysis.

One reason for utilizing definitions of h different from the natural definitions, even for the Paris equation, is for comparison of behavior for various values of N_p . Figure 4 shows time histories for the damage parameter defined as $h = \ln(a)$, the natural definition for $N_p = 2$. Time histories are shown for behavior with values of N_p equal to 1.8, 2.0, and 2.2. The three cases shown have identical initial crack size, and their Paris equation coefficients C_p were chosen to provide identical crack growth rate at the initial time.

2.2 The Statistics of Random Loading

As described in Subsection 1.2, the loading sequence characteristics which have the greatest effect on crack growth are the values of minima and immediately succeeding maxima on the applied stress, s_{\min} and s_{\max} . The most important effect is that of $\Delta s = s_{\max} - s_{\min}$, with the individual values having a secondary effect. The statistical model of the environment encountered by the structure should therefore emphasize these characteristics, even though the corresponding statistics might be much more difficult to establish than other characteristics of the loading.

The Paris model of crack growth utilizes only the values of Δs . For this model, a probability density function of this one variable suffices as a complete loading model. The Forman model and other reasonably realistic models include the effect of the individual values of s_{\min} and s_{\max} on the crack growth rate. Because of the form of the crack-growth models, individual probability density functions of these two variables are not sufficient. At least some information about their correlation is necessary, and a joint density function of the two variables would be especially desirable.

There are three approaches which may be used to determine the desired statistical information about s_{\min} and s_{\max} . The first approach assumes that the loading is Gaussian noise, and attempts to analytically derive the desired statistical information. Given Gaussian loading, s , the individual probability density functions of s_{\min} and s_{\max} are well known [23]. However, the probability density of $\Delta s = s_{\max} - s_{\min}$ depends upon the correlation between each minimum and its associated (immediately succeeding) maximum, and can be obtained only with difficulty by a numerical integration procedure developed by J.R. Rice [24,25,26]. It should be noted that Δs by definition cannot be negative, and

a normal probability density always provides nonzero probability of negative values. Hence, even when the loading is Gaussian noise, the probability density function of Δs cannot be normal. An example of the probability density function of Δs is shown in Fig. 5, for a particular Gaussian noise loading.

The joint density function of s_{\min} and s_{\max} , desired for more realistic crack growth models, is much more difficult to find. The necessary procedures for developing such a joint density function are available [24]. Unfortunately, the procedures include numerical methods because closed-form expressions could not be formulated. Utilization of the procedures requires a substantial effort which must be repeated for each new form of power spectral density considered.

For the present analog simulation effort, maximum use is made of Rice's results without utilization of these procedures. An interim solution for modeling time-histories of s_{\min} and s_{\max} has been developed for use in an analog Monte Carlo approach. Although many approximations and assumptions are made, for simplicity and because of the scarcity of information, the interim model does produce time-histories whose statistics approximate the density functions shown in Fig. 5 reasonably well.

The second approach to the determination of the statistics of s_{\min} and s_{\max} utilizes a Monte Carlo analysis. Gaussian noise with a particular power spectral density is produced on analog computer equipment by driving a linear system with a white-noise generator. The digital portion of a hybrid analog/digital computer then samples the Gaussian noise sufficiently rapidly to determine the occurrences and values of minima and maxima. These values are processed by the digital computer, over a substantial time period, to determine the s_{\min} and s_{\max} statistics. This may not only be more cost-effective than Rice's derivation for the straightforward Gaussian case, but it is much more suitable for extension to more complicated cases. For instance, certain forms of non-Gaussian random loading may be treated, if the loading characteristics are well enough known for appropriate signals to be generated for sampling and statistical processing.

The third approach to the determination of the statistics of s_{\min} and s_{\max} is the most accurate, but depends on the availability of extensive actual load histories. This approach involves examination of the load histories to determine the successive values of s_{\min} and s_{\max} , and inspection of these values to determine their statistics. The loading is not necessarily Gaussian noise; in fact, the investigator need not have any a priori knowledge of the loading

statistics. This makes this third approach the most flexible of all. The steps involved are represented in Fig. 6. As shown, available flight data will give sampled values of flight parameters at discrete times. These data can, for example, be interpolated to provide assumed time histories. The maxima and minima can then be identified, and the important characteristics such as Δs can be established for each loading cycle. (A simpler but still useful approach is to program a digital simulation of a discrimination counter.) These results can then be inspected to determine the statistics of the input to the crack-growth dynamic system.

In previous investigations of the statistics of aircraft loading, there have been attempts to characterize the loading sequence in some analytically describable fashion [4,5]. The stress "s" has been assumed to be a Gaussian processes. This might appear to be a simplification; i.e., an approximation which makes the subsequent utilization of the load model easier. However, there is no resulting simplification because, as described above, it is extremely difficult to derive the statistics of s_{\min} , s_{\max} , etc. from the power spectral density of s, and the resulting statistics are not Gaussian anyway. Therefore, the third approach described above for determination of the statistics of s_{\min} and s_{\max} (i.e., direct inspection of large quantities of flight data) is the method of choice for crack growth risk analyses. This approach avoids both the necessity to analytically describe the loading, and the difficult analytic determination of its important statistics.

The crack-growth dynamic system can be modeled with either load cycles or time (flight hours) as the independent variable. If the system is modeled with load cycles as the independent variable, some correspondence must be established between time and cycles. Fortunately, the number of load cycles per unit time varies little among various samples of the random loading, even though the important characteristics of the loading may vary substantially. Sufficient accuracy might therefore be obtained by utilizing the mean value of load cycles per unit time to transform from the statistics in terms of load cycles produced by the dynamic model, to statistics in terms of flight hours. However, when direct inspection of flight data is used to obtain loading statistics, there is no need to depend upon the expected number of load cycles per unit time. Since the sampled flight data includes time information, the statistics can simply be gathered in terms of occurrences per unit time. Expected total number of

load cycles per unit time may be one of the statistical parameters measured, but it need not be a basis on which all other statistics are dependent for their expression in terms of time.

Consideration of the statistics necessary for accurate determination of the "acceleration effect" provides further reason for obtaining statistics from direct inspection of flight data. The Forman equation (Eq. 13) indicates what the important characteristics of the loading will be for the basic, layering, and acceleration effects. The basic and layering effects merely require some moments of the joint probability density function of s_{\min} and s_{\max} , or perhaps that of Δs and s_{\max} for better accuracy of results. The acceleration effect will require adequate information concerning the occurrences of exceptionally large values of s_{\max} . It is known that a simple Gaussian model for stress "s" will provide inaccurate estimates of occurrences of such large values of s_{\max} [5]. Improved analytically describable models would provide better estimates, but their accuracy would always be questionable. Direct inspection of flight data can avoid this problem, as long as the need for the statistics of large values of s_{\max} is predetermined. The first few moments of the probability density of s_{\max} cannot be expected to provide a sufficiently accurate prediction of the occurrences of exceptionally large values, but separate information concerning level exceedances can be gathered during inspection of the flight data. If the acceleration effect is multiplicative as in the Forman equation, then joint statistics with Δs and s_{\max} must be considered for the level exceedances. However, if the acceleration effect can be modeled as additive, then the statistics of level exceedances may be considered separately from the statistics of Δs and s_{\max} , greatly reducing the complexity of the statistics which must be handled. In order to determine whether an additive acceleration effect models the material behavior sufficiently well, empirical data such as presented in Ref. 20 should be consulted.

Interaction effects between load cycles must also be considered. Load-interaction consists primarily of a reduction in crack growth-rate during the few cycles immediately following the occurrence of a very large maximum stress. When performing cycle-by-cycle analyses, this effect can be modeled by various retardation rules, of which the most accurate [15,16] require current crack-size values for the analysis. However, the effects of retardation can still be incorporated in the load model if suitable assumptions about crack size are introduced.

An illustrative example based on the Willenborg model will be given here. The Willenborg model [15] replaces the applied crack-tip stress intensity factor, K , by an effective factor defined as:

$$K' = K - K_R \quad (18)$$

where

$$K_R = K_{\max}^{\text{OL}} \sqrt{1 - \Delta a / z_{\text{OL}}} \quad (19)$$

and where K_{\max}^{OL} is the maximum stress intensity factor associated with a prior overload cycle, Δa is the crack-size increment between the overload and current cycles, and z_{OL} is a parameter which defines the size of the hardened zone ahead of the crack tip. The latter parameter can be calculated from plastic-zone-size estimates:

$$z_{\text{OL}} \sim (K_{\max}^{\text{OL}} / f_{\text{ty}})^2 \quad (20)$$

where f_{ty} is the material tensile yield strength. The Willenborg model then defines the effective stress range and ratio according to:

$$\Delta K' = K'_{\max} - K'_{\min} = K_{\max} - K_R - (K_{\min} - K_R) = \Delta K \quad (21)$$

$$R' = K'_{\min} / K'_{\max} = (K_{\min} - K_R) / (K_{\max} - K_R) \quad (22)$$

Thus, the procedure for incorporating Willenborg retardation in the load model must preserve Δs while adjusting the stress ratio,

$$R = K_{\min} / K_{\max} = (S_{\max} - \Delta S) / S_{\max} \quad (23)$$

If it is assumed that K is sufficiently insensitive to local geometry effects, the changes in these effects over a few load cycles can be neglected, and Eq. 22 can be reformulated in terms of stress parameters:

$$R' = (S_{\max} - \Delta S - S_R) / (S_{\max} - S_R) \quad (24)$$

where

$$S_R = S_{\max}^{\text{OL}} \sqrt{1 - \Delta a / z_{\text{OL}}} \quad (25)$$

Once s_R has been calculated for the current load cycle, R' can be found and s_{\max} can be adjusted according to:

$$s'_{\max} = \frac{1-R}{1-R'} s_{\max} = \frac{\Delta S}{1-R'} \quad (26)$$

The forward extent of the retardation effect is bounded by

$$\Delta a \leq \Delta a_{\max} = z_{\text{OL}} \sqrt{1 - (s_{\max} / s_{\max}^{\text{OL}})^2} \quad (27)$$

Thus, incorporation of Willenborg retardation in the load model is straightforward, provided that a reasonable method for estimating Δa can be formulated. One possible approach is to include cycle-by-cycle da/dN calculations, using the Forman equation, in the cycle-by-cycle inspection of loads. Since these calculations extend only over one typical set of (say) 50 flights per mission type, the added computational cost is not excessive. The da/dN calculations must be performed in parallel with several initial-crack sizes which represent the entire range of crack size which might be expected in one airplane life (e.g. MIL-A-83444 criteria size to critical size). Obviously, the retardation effect will become less significant late in an airplane life, when the current crack sizes are larger. The gradual disappearance of retardation will be reflected in the statistics of the adjusted load spectra (i.e. s'_{\max} , as given by Eq. 26), and may be thought of as a fictitious usage change for the purpose of random-load crack-growth prediction.

Three approaches are possible for the loads-adjustment procedure. First, one might assume that the effect of each overload extends only to the occurrence of the next overload. In this case, the adjustments of s_{\max} fall into non-overlapping compartments. Second, one might assume that the effect of each overload, extends to the occurrence of the next larger overload, in which case

the compartments overlap partially. Finally, one might assume that retardation is a cumulative effect which applies to all cycles forward of a given overload, subject only to the crack-growth limitation given by Eq. 27. In all cases, the adjustments can be made by appropriately controlled scans of the raw reduced flight data Δs , s_{\max} . Selection of an approach and determination of the number of representative crack sizes required to permit smooth transitions of load statistics over an airplane life are subjects which require additional study. In particular, the latter determination should be based upon the results of calculations with actual flight-loads spectra, especially since the amount of detail required may be sensitive to usage.

2.3 Derivation of Crack-Size Statistics

The analytic prediction of crack growth statistics was considered as an alternative to analog Monte Carlo simulation. If feasible, it would eliminate the necessity of utilizing analog computer facilities. At the very least, this analysis would result in a better understanding of the processes involved, so that analog simulation could be performed both more accurately and more economically.

Analytic prediction of the statistics proved to be quite easy for simple models of loading and crack growth behavior. A FORTRAN program was written to predict the statistics of final crack size for a certain type of crack-growth problem, specifically the problem considered in previous work [19]. The Paris equation is used to model crack growth behavior and the loading is modeled as follows. The total number of loading cycles, N , is given, and these cycles are divided evenly into n blocks. Within each block, the value of Δs is constant. The value of Δs for each block is found by sampling an input noise consisting of white noise and an additive constant. This is an extremely crude model of the statistics of Δs , especially since it even provides nonzero probability of negative Δs , but it suffices for an example.

Since the Paris crack-growth model was utilized with $N_p = 4$, the damage parameter h was chosen as $h = 1/a$, with the rate equation as given by Eq. 4. Since the rate of change of the damage parameter does not depend on its instantaneous value, statistical analysis proceeds with little difficulty. The values of Δs for the various blocks are statistically independent, and they have the same given normal probability density function. All moments of this density function are known, where these moments are:

$$m_p^{(\Delta S)} = E[(\Delta S)^p] = \text{Expected value of } (\Delta S)^p \quad (28)$$

Therefore, the moments of $(\Delta S)^4$ are also known, being given by:

$$m_p^{(\Delta S^4)} = E[(\Delta S^4)^p] = m_{4p}^{(\Delta S)} \quad (29)$$

The total damage sustained by the structure after the N loading cycles, with constant Δs (constant amplitude cycles) within each of the n blocks, is then:

$$\Delta h = - \frac{N}{n} C_p \sum_{i=1}^n (\Delta S_i)^4 \quad (30)$$

It is convenient to define:

$$g = - \frac{\Delta h}{NC_p} = \frac{1}{n} \sum_{i=1}^n (\Delta S_i)^4 \quad (31)$$

which will eliminate confusion in the following analysis. The expected value of g is simply:

$$E[g] = \bar{g} = E[(\Delta S)^4] = m_1^{(\Delta S^4)} \quad (32)$$

The statistics of g are represented by this mean value and by the central moments, which are the moments of the probability density function about \bar{g} . The central moments are:

$$\mu_k^g = E[(g - \bar{g})^k] =$$

$$= \frac{1}{n^k} \sum_{i_1=1}^n \sum_{i_2=1}^n \dots \sum_{i_k=1}^n (E[\prod_{j=1}^k \{(\Delta S_{i_j})^4 - \bar{g}\}]) \quad (33)$$

In general, there are n^k terms to consider. This is excessive, and is reduced by grouping terms of the same type, as described below. The total effect of each group is calculated and added to the effects of other groups, greatly reducing the number of computations necessary.

A "type" is distinguished from another "type" if the expected value of the product:

$$E[\prod_{j=1}^k \{(\Delta S_{i_j})^4 - \bar{g}\}] \quad (34)$$

is not the same. A more useful method of distinguishing between types can be developed. If the indices i_1 through i_k are separated into groups, with identical values grouped together, then there will be γ groups with v_i elements in the i^{th} group. The above expected value can then be written as:

$$E[\prod_{j=1}^k \{(\Delta S_{i_j})^4 - \bar{g}\}] = \prod_{k=1}^{\gamma} \mu_{(\gamma_k)}(\Delta S^4) \quad (35)$$

Therefore, two terms are of the same type if they contain the same number of groups γ , and if the values of v_i are the same. The order in which the values of v_i appear is not important.

A procedure has been developed for finding all possible types of terms and calculating the number of the n^k terms which are of each type, without having to consider the terms individually. The contributions of all types are combined to economically provide the results for the moments of g , which can easily be processed to provide the moments for Δh .

As the number of blocks (n) increases, the probability density of Δh will approach a normal density function. All odd central moments will approach zero, and all even central moments will approach the appropriate values for a normal density function. The amount by which a density function departs from the normal can be represented by its eccentricities, which are defined as:

$$e_n = \mu_n / (\mu_2)^{n/2} \quad \text{for } n \text{ odd}$$

$$e_n = \frac{\mu_n}{(\mu_2)^{n/2}} - 1 \times 3 \times 5 \times \dots \times (n-1) \quad \text{for } n \text{ even}$$
(36)

A probability density function is then completely described by its mean, standard deviation, and its eccentricities of order 3 and higher. Only the first few eccentricities are necessary for a reasonable approximate representation of the statistics, since only the first few are likely to be non-negligible.

A FORTRAN program has been written which provides the mean, standard deviation, and the third and fourth eccentricities (skewness and excess kurtosis) of the probability density function for Δh . This program, using the procedure outlined above, is presented as Appendix A of this report. Some example output from the program is presented as Appendix B.

2.4 Reanalysis of Previous Monte Carlo Simulation

A reanalysis of the previous work [19] on analog Monte Carlo simulation of crack growth has been performed. This reanalysis has revealed some errors in the work, and hence has affected the details of the continued development of the Monte Carlo approach. This reanalysis has also helped to compare the analog Monte Carlo approach with other approaches to the overall problem.

The previous work performed Monte Carlo experiments of fatigue crack growth as follows. White noise, actually limited in frequency but apparently containing high enough frequencies for the purpose, was produced. The noise with an added constant was sampled at intervals, and the value of each sample was held until the next sample time, resulting in a function with steps. This function was assumed to represent the loading parameter Δs in the Paris equation. The dynamics of crack growth as modeled by the Paris equation were then simulated on the analog computer, providing crack size as a function of time. This procedure was rerun many times for the same initial conditions, with varying crack size results because of the randomness of the simulated loading parameter Δs . The varying results were then inspected to estimate the statistics of the final crack size under the simulated conditions.

The previous work used the Paris crack growth model with $N_p = 4$. As has been described, the appropriate choice for the damage parameter in this case is $h = 1/a$, giving

$$\frac{dh}{dN} = -C_p (\Delta S)^4 \quad (37)$$

Consequently, as explained in Subsection 2.3, experiments with the same loading but with different initial values of crack size a_o are identical, when considered in terms of the change in the damage parameter from its initial value, $\Delta h = h - h_o$.

The previous work consisted of two classes of experiments. Both had Δs modeled as sampled white noise with standard deviation $\sigma_{\Delta s}$, and an added constant $\overline{\Delta s}$. Within each class these parameters were the same, but initial crack size was different for the different experiments. Each class can then be considered as a number of identical experiments in Δh , with different scaling factors used in modeling the experiments on the analog equipment.

The experimental data to be reanalyzed were available on punched cards. The data were re-interpreted in terms of Δh providing the following four results for each experiment:

$$\begin{aligned} \overline{\Delta h} &= \text{mean of } \Delta h \\ \sigma_{\Delta h} &= \text{standard deviation of } \Delta h \\ e_3^{(\Delta h)} &= \beta_1 = \text{skewness of } \Delta h \\ e_4^{(\Delta h)} &= (\beta_2 - 3) = \text{excess kurtosis of } \Delta h \end{aligned}$$

The skewness and excess kurtosis represent the amount by which the probability density function for Δh differs from a normal distribution. The above four parameters were computed for four times in the life of each experiment of the previous work (8K, 10K, 13.3K, and 20K cycles).

The means Δh were found to be fairly consistent within each class of experiments. The standard deviations were less consistent, with variations of 20 percent between high and low values not uncommon. The third and fourth eccentricities (skewness and excess kurtosis) were sometimes more than an order of magnitude apart. Considering that each experiment provided about 200 reruns for the data analysis, the experimental procedure must be seriously questioned.

The previous work reported that as the sampling rate was varied up to about 200 Hz, the standard deviation of Δh was reduced. However, as the sampling rate was increased above 200, even to 1200 Hz, the standard deviation did not continue to decrease. This is in conflict with the known results described in the previous subsection, and is therefore another reason to seriously question the experimental procedure. Because of this abnormality, we attempted to reproduce the previous work, utilizing the same electronic equipment. The sample-and-hold circuitry was immediately recognized as the primary cause of the discrepancies.

Figure 7 shows some examples of sampling of white noise using the solid-state sample-and-hold mechanism on the analog computer. Although the white-noise generator appears to be adequate, the samples are obviously correlated (each sample is likely to be similar to the immediately preceding sample). It is known that samples of white noise are completely uncorrelated regardless of the sampling rate. This explains the observed discrepancies in the experimental results.

The prediction method for crack growth statistics described in Section 2.3 was applied to the two classes of experiments. All of the input parameters for the calculation were known except for the number of samples. Sampling was performed at 250 Hz, which would provide (at the four times considered) 40, 50, 66.5, and 100 samples. However, because of the correlations of the samples introduced by the sample-and-hold mechanism, the effective sampling rate was much slower. If the calculations are performed for approximately one fifth the above sample rate (9, 11, 15, and 22 samples at the four times considered), then the experimental and analytical results are fairly consistent. The mean $\overline{\Delta h}$ is consistently about

10 percent higher experimentally than analytically, and since it does not depend on sampling rate this discrepancy is attributed to other analog circuit errors. Comparison of values of $\sigma_{\Delta h}$ also shows good agreement, but of course this agreement is caused by the choice of sampling rate used in the analysis, one-fifth the actual rate. The conclusion to be drawn from this is that the sample-and-hold mechanism introduced a correlation time of about five samples into its output. Inspection of Fig. 7 shows that this correlation time is reasonable.

To summarize, it must be concluded that the previously reported statistics of final crack size were primarily the result of a spurious effect in the analog sample-and-hold device, which was therefore rejected for subsequent work. The problem with the sample-and-hold device was unfortunate, but not serious, since the device had only been utilized as a temporary measure pending more accurate modeling of the loading characteristics. The more accurate modeling has been accomplished by the interim model for time-histories of s_{\min} and s_{\max} mentioned in Subsection 2.2.

2.5 Utilization of Density Moments

As previously described, the analytic derivation of final crack size statistics results in the first few moments of the probability density function of a damage parameter, h . Once these moments have been determined, they must be used to develop a model of the probability density function itself. This will then allow calculation of probabilities of interest, such as structural failure or crack size large enough for visual detection. These probabilities of interest are mathematically represented by inequalities in the damage parameter.

It is not difficult to formulate models of probability density functions which have the specified first few moments. It is much more difficult to formulate such models which are realistic. The first attempt was formulated as:

$$f(h) = \bar{f}(h) \{1 + \alpha_0 + \alpha_1 h + \alpha_2 h^2 + \dots + \alpha_n h^n\} \quad (38)$$

where $f(h)$ is the density function for h , and $\bar{f}(h)$ is a normal density function with the same mean and standard deviation. Unfortunately, although this exactly matches the specified first n moments of the density function, the unspecified higher moments were extremely unusual. The resulting model of the density function appears valid near the mean, but far from the mean the function has

negative values which are physically unrealizable. This approach would therefore be sufficient for computation of exceedance probabilities near the mean. However, more extreme values cannot be evaluated by this approach.

Consequently, another approach must be taken. The second approach considers the log-characteristic function of the probability density,

$$\psi(\omega) = \ln \left[\int_{-\infty}^{\infty} e^{j\omega h} f(h) dh \right] \quad (39)$$

where $j = \sqrt{-1}$. This is simply the logarithm of the inverse Fourier transform of the probability density function. For a normal density, this function is simply a quadratic,

$$\psi(\omega) = j\omega \bar{h} - \frac{1}{2} \omega^2 \overline{h^2} \quad (40)$$

The model to be used for crack-size statistics incorporates a higher-order polynomial in h , which will satisfy specified values of the first few moments, while giving reasonable values for the unspecified higher moments of the probability density of h . This approach has been used previously for similar problems [27].

For example, when the first four moments of a random variable are specified as

$$m_1 = \bar{h} \quad m_2 = \overline{h^2} \quad m_3 = \overline{h^3} \quad m_4 = \overline{h^4} \quad (41)$$

and the higher-order moments are unspecified, the log-characteristic function $\psi(\omega)$ would be a quartic in ω , and the first four moments of h are exactly matched if [28]:

$$\begin{aligned} \psi(\omega) = & j\omega m_1 - \frac{1}{2} \omega^2 m_2 + \\ & - \frac{1}{6} j\omega^3 (m_3 - 3m_2 m_1 + 2m_1^2) + \\ & + \frac{1}{12} \omega^4 (m_4 - 4m_3 m_1 - 3m_2^2 + 12m_2 m_1^2 - 6m_1^4) \end{aligned} \quad (42)$$

However, the computation of the log-characteristic function is only a first step. The desired results are exceedance probabilities for extreme values of h , which will be important in risk analyses. This is theoretically accomplished by applying a Fourier transformation to the exponential of $\psi(\omega)$ to provide the probability density $f(h)$ and then taking appropriate semi-infinite integrals of $f(h)$ to provide the exceedance probabilities. Neither step can be accomplished analytically; numerical methods will be required.

Section III

ANALOG SIMULATION OF CRACK GROWTH

3.1 Results for Specific Tasks

Eight of nine specific analog programming tasks were completed in the present investigation. The following subsections outline each task, describe the procedures used to implement the task on the analog computer, and present the results of test runs. For the purpose of the study, the simulations of all expressions for stress intensity factors have been simplified by omitting the constant factors, i.e. $K = s\sqrt{\pi a}$ for a crack in an infinite plate is replaced by $K \approx s\sqrt{a}$. (in any case, the constant factors would have been absorbed in the Forman equation rate constant, C_F .) All test runs were made on the CI-5000/5 hybrid analog/digital computer at the USAF Aeronautical Systems Division (ASD/ADSD), Wright-Patterson Air Force Base, Ohio.

3.1.1 Forman Equation

Simulation of the Forman equation on the analog computer is a straightforward task. The simulation was programmed in terms of the inverse damage parameter "h" (see Eqs. 12-14 in Subsection 2.1). For the purpose of this study, 7075-T6 aluminum was taken as an example alloy, with experimental growth-rate data [20] fit by:

$$N_F = 3 \quad C_F = 5 \times 10^{-13} \quad K_C = 68 \text{ ksi}\sqrt{\text{in.}} \quad (43)$$

For the special case of $N_F = 3$, Eq. 13 can be simplified to the form:

$$\frac{dh}{dN} = -C' (\Delta S)^2 \quad S_{\max} \left[\frac{S_C}{S_C - S_{\max}} \right] \quad (44)$$

where $S_C = K_C h$ and $C' = (1 - N_F/2) C_F / K_C$.

The analog flow chart for Eq. 44 appears in Fig. 8. Stability and accuracy were checked initially by a simulation with constant-amplitude loading (s_{\min} and s_{\max} held constant, cycles converted to analog computer time by analog scaling laws). An initial condition of $h_0 = 10$ ($a_0 = 1/h^2 = 0.01$ inch) was specified. The solution was stable until a crack size of approximately ($h = 1/\sqrt{a} = 0.5$) was reached.

Typical results of additional tests with random load inputs are illustrated in Figs. 9 and 10. Band-limited white noise with a 350 Hz cutoff frequency was used to model both s_{\min} and s_{\max} . These signals are fully correlated because they were produced from the same noise generator without time-delay. Hence, Δs is still a constant-amplitude signal, as is evident in the figures. However, dh/dt is still a random variable, since s_{\max} appears alone in Eq. 44. No overloads occurred in the analog operational amplifiers when the unfiltered noise input was used. Figure 9 presents a single, real-time solution. Figure 10 illustrates a sequence of solutions with the analog run in its repetitive operation mode. The several replicates run in this mode resulted in identical values of final crack size, the value being in agreement with analytical calculation based on:

$$\overline{(dh/dN)} = -C' (\Delta s)^2 \bar{s}_{\max} \left[\frac{s_c}{s_c - \bar{s}_{\max}} \right] \quad (45)$$

This is in accordance with the property of $\int dh/dN$ (based on the Central Limit Theorem) discussed in Section 2.

3.1.2 Retardation

Retardation models such as the Wheeler model [14] do not account directly for load-interaction effects. The Wheeler model might be applied to the Forman equation by replacing Eq. 9 with:

$$\frac{da}{dN} = \frac{C_F}{K_C} (\Delta s)^{N_F} a^{N_F/2} \left[\frac{s_{\max}}{\Delta s} \right]^m \left[\frac{s_c}{s_c - s_{\max}} \right] \quad (46)$$

The Wheeler exponent, m , can be determined by trial-and-error adjustment until acceptable predictions are obtained for crack size versus cycles by comparison with experimental data for a given load spectrum. It is evident that Eq. 46 can be simulated with no more difficulty than encountered in simulating a general Forman equation. One need only define an appropriate damage parameter and define s_c accordingly. For instance, for $mN_F > 2$, the "natural" definition of the damage parameter is:

$$h = a^{1-mN_F/2} \quad (47)$$

and S_c is then found to be

$$S_c = K_c / \sqrt{a} = K_c h^{1/(mN_F-2)} \quad (48)$$

Hence, the only extra step for a Wheeler-Forman simulation involves the determination of the exponent, m , from laboratory tests.

However, the currently preferred interaction models account individually for the effects of isolated overloads. The present program task required a demonstration of the ability to simulate retardation by isolated overloads, including a gradual return to unretarded growth rates. If one of the accepted interaction models [15,16] is adopted, the simulation then implies that point-calculations of the retardation effect must be made from continuous-function representations of the stress parameters. Such a procedure would undoubtedly increase the analog computing error to unacceptable levels.

Additional insight into the complications involved can be gained by considering a Paris equation, modified by a simplified interaction model. Suppose that

$$da/dN = C_p (\Delta S \sqrt{a})^{N_{P_0}} \quad (49)$$

in the absence of overloads, but that:

$$da/dN = C_p (\Delta S \sqrt{a})^{N'_P} \quad (50)$$

$$N'_P = N_{P_0} (1 - e^{-\Delta N / \bar{N}}) + N_{P_1} e^{-\Delta N / \bar{N}} \quad (51)$$

replaces Eq. 49 immediately after an overload. In Eqs. 50 and 51, the cycle count ΔN begins at zero on the cycle immediately following the overload, and N_{P_1} , \bar{N} are assumed to be given quantities with $N_{P_1} < N_{P_0}$. Hence, the retardation effect appears as a series of step-drops followed by exponential rises in the growth-rate exponent. One can conceive of simulating this model on the analog. However, there is no longer any unique relation between crack size and the damage parameter:

$$h = a^{1-N'_P/2} \quad (52)$$

Therefore, a simulation directly in terms of crack size would be required. Furthermore, the principal advantage of the analog (using a short period of computing time to represent a large number of load cycles) is lost because of the need to represent the individual overload cycles. Thus, if time-compression is used, many isolated overloads appear lumped together in the stress-parameter signals, and Eq. 50 is activated too infrequently. Similar conclusions can be drawn about simulation of the Forman equation with an accepted retardation model. Therefore, retardation models were not implemented on the analog computer.

3.1.3 Local Geometry Effects

The third programming task was to demonstrate the ability to vary a simulated crack growth rate by including a local geometry effect, e.g. the change in stress intensity factor for a crack which grows away from a fastener hole. The geometry effect can be expressed in terms of a dimensionless parameter, β , such that the effective range in stress intensity factor is given by:

$$\Delta K_{\text{eff}} = \beta \Delta K \quad (53)$$

The parameter, β , can usually be stated in terms of the ratio of crack size to a significant dimension associated with the geometry of a local structural detail. However, β cannot always be expressed analytically. For example, β is a function of a/r for a crack growing away from a fastener hole, where r is the radius of the hole. If the hole is open and is located in a large panel subjected to uniform edge tension, and if the crack orientation is perpendicular to the tension, then $\beta \approx 3.4$ for very small cracks ($a/r \rightarrow 0$) and $\beta \rightarrow 1/\sqrt{2}$ as $a/r \rightarrow \infty$, according to a complex variable solution by Bowie [29]. This and many other numerical solutions for β associated with other simple geometries are available in graphical form [30]. For more complicated geometries, β can be obtained by finite-element analysis, e.g. using hybrid-stress crack-tip elements [31].

If the local geometry effect is included in the Forman equation, the crack growth-rate becomes:

$$\frac{da}{dN} = \frac{C_F (\beta \Delta K)^{N_F}}{(1-R) K_C - \beta \Delta K} \quad (54)$$

Note that $R = K_{\min}/K_{\max}$ is not affected by β . Equation 54 can then be transformed into:

$$\frac{dh}{dN} = \left(1 - \frac{N_F}{2}\right) \frac{C_F}{K_c} (\beta \Delta S)^{N_F} \left[\frac{S_{\max}}{\Delta S}\right] \left[\frac{S_c}{S_c - \beta S_{\max}}\right] \quad (55)$$

where $\Delta K \approx \Delta S \sqrt{a}$ has been assumed as before. In principle, β can be described directly in terms of the damage parameter, rather than crack size.

In the present study, the empirical finite-width correction factor:

$$\begin{aligned} \beta = 1 + 1.1896\lambda^2 + 1.3016\lambda^4 + 1.3650\lambda^6 + \\ + 1.3739\lambda^8 + 1.4764\lambda^{10} \end{aligned} \quad (56)$$

was chosen for implementation. Equation 56 represents the accelerating effect of a single edge-crack of length, a , growing across a plate of width, b , with the plate subjected to uniform tension, and with $\lambda = a/b$. Thus, one could calculate λ continuously on the analog by substituting the damage-parameter transformation to obtain:

$$\lambda = \frac{1}{b} h^{2/(2-N_F)} \quad (57)$$

However, a function-generation approach is obviously more convenient and more economical in terms of the number of analog components used. Most modern analog computers include function generators which nominally provide piecewise linear representations for functions of one input variable, with ten to twenty segments allowed. Equation 56 provides a severe test of this capability because of the strong nonlinearity in β . Figure 11 compares Eq. 56 with a typical representation obtained on the analog. In this case, the simulation has been formulated in terms of $1/\beta$ to avoid numerical instability in the function generator. The points were selected for segment generation for a plate width $b = 10$ inches and rate exponent $N_F = 3$, as follows:

Crack Size, a (inch)	Function Input, $h=1/\sqrt{a}$ (in. ^{-1/2})	Function Output, $1/\beta$
0.01	10	1.0000
0.01562	8	1.0000
0.04	5	1.0000
1.0	1	0.9743
1.235	0.9	0.8797
1.562	0.8	0.5709
2.041	0.7	0.2010
2.778	0.6	0.0467
4.0	0.5	0.0078
10.0	0.316	0.0000

The above table suggests that the crack-growth simulation would probably have to be restricted to a maximum crack size between 1 and 2 inches for this case. Figure 11 illustrates the limitation of the analog's ability to match a severely nonlinear function.

With regard to implementation of a geometry factor in the Forman equation, it is apparent that β can be inserted in the appropriate places in the flow chart shown in Fig. 8, with the aid of several additional multipliers. One multiplier is required to form the product βs_{\max} just before the inverter which outputs $s_c - s_{\max}$, while three multipliers are required to form β^3 and then the product $\beta^3 \Delta s^2$ near the upper center of the diagram. The solution-instability problem will not exist for other types of geometry factors, such as β for a crack growing away from a fastener hole. Also, the exact function will be easier to match because the nonlinearity is much less severe.

3.1.4 Randomized GAG Sequence

For the purpose of predicting crack growth a GAG cycle can be treated as having two components, both of which result from the sudden change in mean stress as an airplane takes off or lands. For example, when the airplane taxis and during the pre-takeoff roll, a point on the lower skin of the wing experiences small-amplitude stress oscillations about a negative (compression) mean. As the airplane approaches takeoff speed, the wings bear an aerodynamic lift which approaches the aircraft weight and reverses the sign of the wing static bending

moment. Following takeoff, the wing lower skin experiences somewhat larger stress oscillations about a positive mean. One can thus identify two effects on crack growth. First, the initial change in mean stress is equivalent to a single, relatively large range at the beginning of each flight. The magnitude of the GAG range can be treated as deterministic (effect of mean only), as a deterministic range from last taxi minimum to first gust maximum, or as random with a small variance equal to the sum of the variances associated with taxi and gust loads. The second effect is that the change in mean stress must be accounted for in the flight-loads cycles. This effect of the mean change on the two-parameter load model is that the values of s_{\max} increase after takeoff, while the values of Δs are not directly affected by the GAG event.

The fourth programming task required a demonstration of the ability to randomize the sequence and time of appearance of a limited number of GAG ranges having deterministic magnitudes. This task was easily accomplished by using band-limited zero-mean Gaussian noise as a switching input summed with an adjustable bias voltage, $-\alpha$, to make the signal mean negative. With an electronic comparator set to switch "on" when the total switching voltage exceeds zero, a constant voltage Δs_0 can be added intermittently to the continuous signal $\Delta s(t)$ which represents flight-loads stress ranges. Figure 12 illustrates the required analog flow chart.

The average number of inputs of Δs_0 per second can be estimated from the expected number of upward crossings of zero by the switching signal [32]:

$$\epsilon(0) = \frac{1}{2} \frac{\overline{v}_0}{\sigma} e^{-\alpha^2/2\sigma^2} \quad (58)$$

where

$$\sigma^2 = \int_0^\infty G(f) df \quad (59)$$

$$\frac{\overline{v}_0}{\sigma} = \frac{2}{\sigma} \left[\int_0^\infty f^2 G(f) df \right]^{1/2} \quad (60)$$

and where $G(f)$ is the power spectral density of the Gaussian noise in units of (volts)²/Hz. For band-limited white noise, Eqs. 59 and 60 are easily evaluated, resulting in:

$$\bar{v}_0 = 2f_c/\sqrt{3} \quad (61)$$

where f_c is the cutoff frequency. The value of α can then be determined from Eq. 58 to provide the proper average time between GAG cycles.

Figure 13 illustrates some typical results from a series of test runs in which $\Delta s(t) = 0$ to isolate the effect of Δs_0 . The bias voltage, α , was varied from -1.51 to -0.91 volts, with $\Delta s_0 = 10$ volts. The Gaussian noise switching input is shown as $x(t)$, and has 1 volt rms with a 350-Hz cutoff ($\sigma = 1$, $\bar{v}_0 = 405 \text{ sec}^{-1}$).

The increase of average time between GAG cycles with decreasing α is evident. The GAG cycle values appear to be random only because the pen-chart recorder response is not rapid enough to reproduce Δs_0 faithfully. The actual Δs_0 can easily be varied over a small range to represent the random effect of first-gust-peak/taxi-minimum by adding a small-amplitude low-frequency sinusoidal signal to Δs_0 .

3.1.5 Superposition of Random Flight Loads and GAG Cycles

The fifth programming task required a demonstration of the ability to simulate the second effect of the GAG cycle, i.e. the change in mean stress (and s_{\max}) following takeoff and landing. The implementation of this task requires two comparators and a time clock. The time clock must be synchronized with the start of the problem solution. Therefore, one simply arranges to compute:

$$t' = c \int_0^t d\tau \quad (62)$$

on the analog, where t represents the current analog time and C is a scaling factor chosen for convenience (to prevent the clock from saturating).

If the two comparators are fed with constant switching voltages t'_1 and $t'_2 > t'_1$, they can be used to choose between three load environments, with the selection changed at computing times $t = t'_1/C$, t'_2/C . The analog circuit shown in Fig. 14 provides such a choice between three random signals which have (in general) different means and different variances. The output signal $s(t)$ might then be used to simulate s_{\max} . Figure 15 illustrates the performance of this circuit with the analog in repetitive operation mode..

3.1.6 Random Initial Condition

The sixth programming task required a demonstration of the ability to simulate a suitable distribution of initial-crack sizes. Such a distribution would be sampled infrequently (once per simulated airplane life) to provide the initial conditions for a Monte Carlo simulation. A non-Gaussian model is desired because initial-crack size distributions are usually skewed.

This task is implemented by using an appropriately shaped zero-mean white-noise source. The shaping function is derived simply as:

$$A(x) = f(x)/\phi(x) \quad (63)$$

where

- $x = x(t)$ = Noise signal
- $A(x)$ = Required shaping function
- $f(x)$ = Sought-for probability density of output
signal amplitudes
- $\phi(x)$ = Probability density of input noise amplitudes

In the present case, $\phi(x)$ corresponds to a Gaussian source with prescribed rms voltage, σ ,

$$\phi(x) = \frac{1}{\sigma\sqrt{2\pi}} e^{-x^2/2\sigma^2}; \quad -\infty < x < \infty \quad (64)$$

while a two-parameter Weibull distribution was sought for the output noise:

$$f(x) = \frac{\alpha x^{\alpha-1}}{\beta^\alpha} e^{-(x/\beta)^\alpha}; \quad 0 \leq x < \infty; \quad \alpha, \beta > 0 \quad (65)$$

Hence the required shaping function becomes:

$$A(x) = \frac{\alpha\sigma\sqrt{2\pi}}{\beta^\alpha} |x|^{\alpha-1} \exp \left\{ \frac{x^2}{2\sigma^2} - \left(\frac{|x|}{\beta} \right)^\alpha \right\} \quad (66)$$

Note that the shaping function must be symmetric about $x = 0$ to account for the restriction of the output to positive values.

Figure 16 compares the required shape with a gain function actually obtained from one of the analog function-generator components. The required shape is intended to produce a Weibull distribution with $\alpha = 2.5$ and $\beta = 0.007$ from Gaussian noise with $\sigma = 0.1$. This is another case where the analog component has difficulty in following a severely nonlinear function. (The gain function shown was obtained only after seven function-generator circuits had been tested for accuracy and rejected.)

The eighth gain function obtained (Fig. 16) was given an accuracy test by sampling the noise signal 1,000 times at sampling rates of 50, 100 and 200 Hz. The 1,000 sample values in each case were then used to obtain maximum-likelihood estimates for the output distribution parameters, according to [33]:

$$\alpha = \frac{N \sum_{i=1}^N x_i^\alpha}{N \sum_{i=1}^N x_i^\alpha \ln x_i - \left(\sum_{i=1}^N x_i^\alpha \right) \left(\sum_{i=1}^N \ln x_i \right)} \quad (67)$$

$$\beta = \left[\frac{1}{N} \sum_{i=1}^N x_i^\alpha \right]^{1/\alpha} \quad (68)$$

where N is the total number of samples. The results obtained were as follows:

SAMPLING RATE (Hz)	MAXIMUM-LIKELIHOOD ESTIMATES FOR:	
	Shape Parameter, α (Required Value=2.5)	Scale Parameter, β (Required Value=0.007)
50	2.01	0.0073
100	2.63	0.0071
200	2.84	0.0069

The above results indicate that there may be some difficulty in maintaining the distribution shape parameter at the much lower sampling rate which would correspond to one simulated airplane life.

3.1.7 Simulation of Random Maneuver Loads

The production of random noise to simulate stress time-histories is a task similar to the simulation of a random population of initial-crack sizes. The

programming task requires a simulation of a non-Gaussian process, such as might represent fighter maneuvering loads.

In this case, it was decided to produce Rayleigh noise:

$$f(x) = \frac{x}{\sigma^2} e^{-x^2/2\sigma^2}; \quad 0 \leq x < \infty \quad (69)$$

Equation 69 also describes a Weibull distribution for the special case $\alpha = 2$, $\beta = \sigma\sqrt{2}$. The shaping function required to produce Rayleigh noise from zero-mean Gaussian noise is:

$$A(x) = \frac{\sqrt{2\pi}}{\sigma} |x| \quad (70)$$

Hence, the shaping filter can be simply constructed with a constant gain, two inverters and a diode, as shown in Fig. 17.

A sampling experiment similar to the one described in Subsection 3.1.6 was conducted, using a 1-rms Gaussian source, with the following results:

SAMPLING RATE (Hz)	MAXIMUM-LIKELIHOOD ESTIMATE FOR:	
	Shape Parameter, α (Required Value=2)	Scale Parameter, β (Required Value= $\sqrt{2}$)
50	1.92	1.43
100	2.04	1.50
200	2.18	1.54

In this case, the shape parameter appears to be less sensitive to the sampling rate, probably because of the linearity of the shaping function.

3.1.8 Incorporation of Threshold Effect

The eighth programming task required incorporation of logic circuitry in the Forman equation to recognize when ΔK is less than a prescribed threshold value below which crack growth is assumed not to occur. When the Forman equation is employed, the threshold value is commonly assumed to depend upon the stress ratio, e.g.:

$$\Delta K_{TH} = (1-R) \Delta K_{TH}^O \quad (71)$$

where ΔK_{TH}^O is a material property measured in a zero-to-tension ($R = 0$) crack-propagation test. However, the stress-ratio effect on threshold was ignored in the present study, i.e. $\Delta K_{TH} = \Delta K_{TH}^O$ was assumed.

The threshold effect is easily implemented by placing an electronic comparator between the gain, C' , and the integrator which outputs the damage parameter, $-h$ (lower left in Fig. 8). With the switching function $\Delta s/h - \Delta K_{TH}^O$ supplied to the comparator, the input to the integrator can be switched between Eq. 13 when the threshold is exceeded and zero when ΔK is below the threshold. A partial flow chart for the additional circuitry is illustrated in Fig. 18.

An example real-time simulation of the Forman equation with the threshold effect was run with loading in which s_{min} was held constant, while s_{max} was modeled by white noise to randomly trigger the threshold. The results are shown in Fig. 19, which records the switch output and $\Delta K(t)$. It is evident that the rate equation spends more time in the circuit as crack size increases, until virtually all ΔK values contribute to crack growth. Also, it is apparent that an equivalent simulation can be implemented with ΔK_{TH} as given by Eq. 71, since the term $1-R$ can be produced as $s_{max}/\Delta s$ using one additional "X/Y" component.

3.1.9 Coupled Dynamics for Two Cracks

The final programming task required a demonstration of the ability to simulate the simultaneous growth of two or more cracks with the rate equations coupled through change of stress intensity near one crack as a function of the size of the others. Situations of this type may occur in aircraft structures, e.g. for two cracks 180° apart growing away from the same fastener hole.

In the present study, a simplified situation was formulated strictly for the purpose of demonstrating the coupling effect without introducing the complications associated with local geometry factors. Suppose that two panels in parallel, of widths L_1 and L_2 , are loaded such that both panels are subjected to the same elongation. Let the panels contain edge-cracks of lengths a_1 and a_2 , and assume for the purpose of the demonstration that the panel compliances are concentrated in narrow strips near the cracks. Then the stress levels in the two panels are given approximately by:

$$s_1 = \frac{P(L_1 - a_1)/L_1}{(L_1 - a_1)t_1 + (L_2 - a_2)t_2} \quad (72)$$

$$s_2 = \frac{P(L_2 - a_2)/L_2}{(L_1 - a_1)t_1 + (L_2 - a_2)t_2} \quad (73)$$

where P is the total load applied to the two panels and where t_1, t_2 are the panel thicknesses. The problem is obviously artificial, but still serves to test the ability of the analog to simulate coupled Forman equations.

For the case $L_1 = L_2 = L$, $t_1 = t_2 = t$ and $N_F = 3$, the rate equations can be expressed as:

$$\frac{dh_i}{dN} = -\frac{1}{2} \frac{C_F}{K_C} [F_i(h_1, h_2) \Delta P]^2 [P_{\max} F_i] \left[\frac{S_{C_i}}{S_{C_i} - P_{\max} F_i} \right]; \quad i=1,2 \quad (74)$$

where

$$F_i(h_1, h_2) = \frac{(L - 1/h_i^2)/Lt}{2L - 1/h_1^2 - 1/h_2^2}; \quad i=1,2 \quad (75)$$

The loading is described by the parameters P_{\max} and $\Delta P = P_{\max} - P_{\min}$. The analog flow chart appears in Fig. 20.

Debugging of this simulation was difficult, due to the instabilities caused by the $1/h_i^2$ terms in the equations. However, two simulations were successfully completed using 7075-T6 properties ($N_F = 3$, $C_F = 5 \times 10^{-13}$, $K_C = 68 \text{ ksi } \sqrt{\text{in.}}$). In the first simulation (Fig. 21), the initial conditions were 0.01- and 0.01888-inch cracks ($h_1 = 10$, $h_2 = 7.3$). (The values of the constants C'_1, C'_2 are equal to $C_F/2K_C$ times the analog scale factor.) In the second simulation (Fig. 22), the initial conditions were equal-sized cracks, while the growth rate of the second crack was arbitrarily increased by a factor of three ($C_F = 1.5 \times 10^{-12}$). In both cases, the panel dimensions $L_1 = L_2 = 10$ inches and $t_1 = t_2 = 0.1$ inch were used, while constant-amplitude loading with $\Delta P = P_{\max} = 140 \times 10^3$ lbs. was chosen. In each case, the crack which grows faster is observed to decelerate toward the end of life, while the slower crack accelerates. This effect results from the transfer of load from the panel with the larger crack to the panel with the smaller crack because of the difference in panel compliance.

3.2 Evaluation of Results

The results of the simulation exercises indicate that the analog approach to crack-growth prediction possesses some advantages and some disadvantages with respect to digital simulation. Generally, the analog can accommodate

random-process driving functions more conveniently, while the digital computer is superior for the simulation of details.

The Forman equation was easily implemented on the analog for the special case of a growth-rate exponent $N_F = 3$ (representative of aluminum alloys). Formulation in terms of the inverse damage parameter "h" makes the simulation stable and permits studies of cracks growing between 0.01 and approximately 4 inches. Random-process drivers can be simulated directly by band-limited white noise, with or without shaping filters to change the probability density function. Simulation of other materials with fractional rate exponents N_F is possible in principle by using the log-antilog components available on the analog patchboard. However, these components are essentially specialized function-generators, and the effects of their possible inaccuracies have not been assessed quantitatively for the crack-growth problem.

With regard to retardation effects, it is apparent that a digital simulation will be superior. Although the Wheeler retardation model can be simulated on the analog (again, at the price of using log-antilog components), any attempt to treat the more sophisticated load-interaction models forces the simulation toward long computing times because of the need for cycle-by-cycle detail in the stress-parameter signals.

Local geometry effects for two-dimensional cracks appear to be amenable to analog simulation by using a piece-wise linear function-generator with one independent variable (a standard patchboard component). A reasonable simulation of one such factor was achieved for a very severe case involving unbounded increase of the stress intensity factor as a crack grows across the finite width of a plate. Simulations of stable geometry effects, e.g. for a crack growing away from a fastener hole, will be much easier. Again, the digital computer is superior in comparison to existing Air Force analog hardware for the simulation of geometry factors for three-dimensional cracks, which require two input variables. However, commercial analog hardware is available for this task (see Subsection 3.3).

Analog simulation of the effects of GAG cycles has been shown to be feasible. Separate simulations were implemented for the isolated large stress range associated with each takeoff, and for the effect of the change in mean stress from taxi to flight loads.

Investigation of the use of shaping filters indicated that both Rayleigh and Weibull processes could be produced from the band-limited Gaussian noise sources available on the analog. However, the results of the tests also indicated some difficulty in accurately reproducing the desired shape parameters for these distributions. Further tests are required to assess the crack-size inaccuracies which might result from inaccuracy of the process shape parameter.

The threshold stress intensity effect was simulated successfully with no difficulty. However, analog simulation of the threshold effect cannot be extended to include the "shutoff" phenomenon, which may occur when load-interaction effects are properly accounted for.

Finally, it has been shown that coupled crack dynamics can be simulated on the analog. However, there is no reason why an equivalent digital simulation could not be implemented.

In summary, the results of the analog simulations indicate that the analog computer provides about the same level of capability as the digital computer, but with some important differences in detail. Hence, there appears to be no overwhelming reason to convert from the digital to the analog approach to crack-growth prediction, especially since many digital programs have already been developed, and in view of the fact that many structural engineers are unfamiliar with analog programming techniques.

3.3 Equipment Availability

In recent years the usage of existing analog and hybrid computers and the demand for new machines has declined significantly. Complete listings of present day manufacturers of hybrid computers are difficult, if not impossible, to obtain. A request for information sent to the six manufacturers listed in the 1972 edition of the Computer Yearbook yielded only two responses (see Appendix C). Some or all of the companies that did not respond may no longer be in existence.

Fortunately for the analog/hybrid user, the responding manufacturers have continued to improve and refine their products. In particular Electronics Associates, Inc. has added multivariable function-generators to their line of products and accessories. Although digital multivariable function generators have been in use for some time, the EAI function-generator employs analog computation between function break points. The multivariable function generator acts independently of the digital central processor and thus achieves a combination of speed and accuracy.

Appendix D compares the features of available new machines with the existing CI-5000/5 computer at Wright-Patterson Air Force Base. Although some of the conveniences and more advanced design philosophies of today's new machines are not reflected in this table, the basic features required for solving the problems discussed in this report are listed. The existing Wright-Patterson hybrid computer compares favorably on all requirements, with the exception of multivariable function-generators.

Section IV

CONCLUSIONS AND RECOMMENDATIONS

4.1 Summary

The results of a program to develop an efficient approach to the risk analysis of random-load crack growth have been presented. The two major objectives of the program were to implement certain specific simulations of crack growth on hybrid analog/digital hardware, and to develop an improved approach to the modeling of random loads.

Under the first objective, eight of nine specific simulation tasks were implemented and verified on analog/digital hardware available at the USAF Aeronautical Systems Division computing facility (ASD/ADSD). These simulations were achievable well within the existing hardware capability (i.e., numbers of multiplier, summation, integrator circuits, etc.) with one exception. The exception is the geometry factor required for stress-intensity calculations associated with three-dimensional cracks. Calculation of this factor requires a function-generator with two independent variables; commercial hardware possessing this capability has been identified.

The ninth task involved load-interaction (retardation) effects and could not be fully implemented as an analog simulation. The Wheeler retardation model could be simulated by using logarithm and anti-log circuits, but the accuracy of these circuits is questionable. Attempts to formulate the more refined cycle-by-cycle retardation models were completely unsuccessful because of the difficulty in extracting the discrete information required for calculating retardation from the continuous simulation of stress time-history.

Under the second objective, a general procedure has been proposed for characterizing random loads from surveys of recorded flight data, in terms of those load statistics which influence crack growth most significantly. In the course of this development, a general study of how to formulate the problem of predicting crack growth due to random loads led to two improvements in the approach. First, the crack growth-rate equations were reformulated in terms of a damage parameter inversely related to crack size. Second, the "estimation theory" developed by modern theorists in guidance and control has been considered for crack growth prediction to obtain a more efficient numerical approach to risk analysis, as described in the following subsection.

4.2 Estimation Theory for the Prediction of Crack-Growth Statistics

In the course of investigating modeling methods for load statistics, the usefulness of estimation theory for application to crack-growth risk analysis was identified. Estimation theory [21,22] is concerned with the analysis of the states of dynamic systems, where such states are not accurately known for three reasons. First, the initial conditions of the system may not be accurately known. Second, the dynamic system is affected by input noise. Third, measurements of the state are also affected by noise, so direct observation of the state is not possible. Because the states are not accurately known, they can only be described statistically. A diagram of this situation is presented in the upper portion of Fig. 23. It should be noted that the noises, states, and measurements shown in the figure are vector quantities, not merely scalars.

It is convenient for the purposes of the estimation theory to represent the dynamic system in "state-space" formulation. The differential equations of the dynamic system, of total order n , can always be rewritten as n first-order differential equations in terms of n variables. These n variables are collected in the "state vector" $\{x\}$. The system equation can then be written as

$$\begin{array}{ccc} \frac{d}{dt} \{x\} = \{f(\{x\})\} + [G(\{x\})] \{w\} & & (76) \\ \text{"state"} & & \text{"white"} \\ \text{vector"} & & \text{noise"} \end{array}$$

For the case of a linear system, $\{f(\{x\})\}$ is simply linear in $\{x\}$, and $[G(\{x\})]$ is constant, so that the system equation can be written as

$$\frac{d}{dt} \{x\} = [F]\{x\} + [G]\{w\} \quad (77)$$

It must be noted that the block diagram of the system shown at the top of Fig. 23 has Gaussian noise input, while the equations shown above allow only for "white noise" (Gaussian noise with flat power spectral density). This discrepancy is easily handled because any Gaussian noise can be produced by passing white noise through an appropriate linear filter. As shown in the lower diagram, an "augmented system" can be developed, with an "augmented state vector" including the states necessary to represent the dynamics of the "input noise filter". The augmented problem is then appropriate for treatment using the equations shown above.

The development of estimation theory began with consideration of steady-state (stationary) behavior of linear systems, with all variables having Gaussian statistics. This restricts the problem represented by Fig. 23 in three ways. First, the system equation can be expressed as in Eq. 77, which restricts the system dynamics to be linear and the noise input to be Gaussian. Second, the matrices $[F]$ and $[G]$ are not time-varying, which restricts the system and the noise input to be both stationary. Third, the system has reached a steady state, or in other words enough time has passed for the initial conditions to have long ceased to have an effect on the problem. This restrictive form of estimation theory is not applicable to the crack-growth problem, which is an entirely transient problem without a steady state.

Estimation theory was then extended to consider non-steady-state (non-stationary) situations, but the models of the system and noise remained linear and Gaussian. The initial conditions of the system became important. This led to the development of the Kalman filter for estimation of the state of a system. Referring again to Fig. 23, the Kalman filter (measurement filter) keeps track of the statistics of the state variables, which are entirely represented by their vector of means and matrix of covariances, since all statistics are assumed Gaussian. The Kalman filter updates these statistics based on a number of effects. First, the system dynamics cause the expected value of the state to change, with corresponding changes in the covariances. Second, the noise input to the system increases the uncertainty of the states, which is realized as an increase in the covariances. Third, the measurements provide information which is useful in better estimating the expected value of the states. Based on the relative accuracy of the measurements (as described by the measurement covariances) and the accuracy of the current estimate of the state (as described by the state covariances), an adjustment of the expected values of the states is made towards the measured values, and the increased accuracy of the estimate is realized as a decrease in the state covariances.

The Kalman filter has been extremely valuable in situations where the best estimate of a state variable was very important, but accurate measurements of that state variable were not available. For instance, navigation of a vehicle is often dependent on noisy (inaccurate) position measurements, especially when operating away from regular routes. In such a situation, the Kalman filter can greatly improve the estimate of current position and heading. In the utilization of the Kalman filter, the greatest difficulty occurs in accounting for the measurements. The propagation of the statistics of the state, considering the system dynamics and the Gaussian noise input, is straightforward.

Many attempts have been made to extend estimation theory to cases of nonlinear systems or linear systems with non-Gaussian statistics, but these were not entirely successful. Jazwinski [21] says that

"Using linearization of one sort or another, Kalman-like filtering algorithms were developed and applied to nonlinear problems. This statistical work received its impetus from the aerospace dollar. Work was duplicated, triplicated; everyone derived his own Kalman filter, perhaps partly because of a lack of understanding of Kalman's original work."

It was soon learned that development of estimation procedures for non-Gaussian statistics and nonlinear systems required a much deeper understanding of the fundamental probabilistic structure of the estimation problem, than did the development of the Kalman filter. This fundamental probabilistic structure is now more completely understood, but estimation of non-Gaussian statistics with nonlinear dynamic systems is still not commonly performed because of the immense computational difficulties involved. First, the means and covariances of the state variables no longer completely define their statistics. An infinite number of statistical parameters would theoretically be necessary to completely define the statistics. However, as long as the random variables are defined so their statistics are not far from normal, a small number of these parameters (such as the first few moments of the probability density functions) can serve as a useful approximation to the complete statistics. The number should be kept as small as possible since each additional parameter disproportionately increases the amount of information that must be carried throughout the computations.

The system dynamics, which are now considered to be nonlinear, also theoretically require an infinite number of parameters to completely specify their behavior. However, the forms of $\{f(\{x\})\}$ and $[G(\{x\})]$ are usually provided with sufficient accuracy by closed-form expressions. In the development of the propagation of the statistics for the nonlinear non-Gaussian system, the dependence of these system dynamic descriptors will be approximated by taking the first few terms of their Taylor series expansion in the states, about the means of the states.

For the linear Gaussian case, it was pointed out that consideration of measurements greatly increased the complexity of the filter. For the nonlinear non-Gaussian case, this increase in complexity is magnified many times over. Fortunately, treatment of measurements will not be part of the crack-growth problem being considered.

The propagation of the first few moments of the probability density of the state for the nonlinear non-Gaussian case is substantially more complicated than for the linear Gaussian case. However, it is a straightforward calculation which can be implemented on a digital computer. There are a number of effects, not present in the linear Gaussian case, which may be important. First, the effect of the nonlinearity of the system cannot be approximated by merely linearizing about the mean value of the states, because this would ignore the very important variations in how the system operates on other-than-average values of the states. Second, the analysis must consider more than the first two moments of the probability density (mean and covariance) even if they are the only results desired, because in the presence of the system nonlinearities higher density moments will affect the propagation of the lower moments. Third, the non-Gaussian statistics of the initial conditions must be considered. Fourth, the non-Gaussian statistics of the input noise should be considered. This fourth effect is probably the least important because the input noise effects are averaged over the time period of concern, but even this effect should not be ignored unless examination of the particular problem shows it to be unimportant.

The problem of predicting crack-growth statistics can now be put in the context of estimation theory. It will be necessary to model the behavior of crack growth by a dynamic system, and to model the important effects of the loading of the structure by a random noise input. It will also be necessary to consider the dynamic system as nonlinear, and the statistics of the noise and state variables as non-Gaussian.

While Gaussian statistics can be completely represented by the first two moments of the probability density (mean and covariance), non-Gaussian statistics generally require an infinite number of statistical parameters to completely represent them. The non-Gaussian statistics are therefore approximated by taking only the first few density moments (perhaps the first four). This approximation will be reasonable only if the higher-order moments do not have significant effect, which is equivalent to saying that the statistics are not far from Gaussian. This will usually be the case if and only if the system dynamics

are not far from linear. Unfortunately, the dynamics of crack growth are highly nonlinear if they are formulated with crack size itself as a state variable, as explained in Subsection 2.1. The solution as presented there is to reformulate the crack-growth dynamics in terms of a damage parameter "h". As was shown in Figs. 1 and 2, this results in a linear dynamic system for the simple case of the Paris crack-growth equation, and a near-linear system for more realistic models such as the Forman equation. Without the use of this damage parameter, the employment of the first few probability density moments to approximate the nonlinear statistics would be inadequate, and the use of a sufficient number of moments would be unrealistically complicated.

Even with the necessity to consider the nonlinear and non-Gaussian situation, the major difficulty of the associated estimation theory is avoided by the crack-propagation problem being considered here. This difficulty is the treatment of measurements, which do not exist in the prediction problem. Without measurements, the nonlinear non-Gaussian situation, which has been either avoided or implemented only at extreme cost by investigators considering other problems, becomes feasible. An additional factor which makes it feasible to handle this situation is that the computations will be performed on large-scale ground-based computers, while many applications of estimation theory have required that computations be performed in real time on much more limited on-board computers.

The system dynamics representing the behavior of crack growth are relatively easy to develop. Available crack-growth models such as the Forman equation are utilized, with the necessary transformation to model the behavior in terms of a damage parameter "h".

The input noise to the dynamic system models the essential characteristics of the loading experienced by the structure, such as stress range Δs and peak stress s_{\max} . The treatment of complex effects, such as retardation, may be included in the development of the input noise model, as was described in Subsection 2.2.

The statistics of the initial conditions of the system (corresponding to the initial-crack sizes) must also be modeled. The initial-crack sizes are usually quite small, with some occurrence of larger initial defects. The probability density function of initial-crack size might very well appear as shown in Fig. 24, with two peaks (a bimodal distribution). This type of

density is not well represented by its first few moments. However, bimodal distributions can be handled by considering the density to be the sum of two separate densities, as shown in the figure. The two densities are utilized as initial conditions for two separate analyses, and the results of the separate analyses are then combined. This illustrates the capability of handling a multi-modal density function accurately, while still approximating the non-Gaussian statistics by only the first few moments of the density function.

4.3 Discussion and Conclusions

Although eight of nine analog simulation tasks were successfully implemented, evaluation of the computing performance indicated that the analog approach to cycle-by-cycle or flight-by-flight crack growth prediction does not achieve any real improvement in computing efficiency, in comparison with equivalent digital computer codes. The inability of analog equipment to process high-frequency signals implies long computation time for one airplane life. Also, analog-circuit errors are significant enough to require repetition of the analysis several times, simply to assess the error in crack size for a deterministic load history. If Monte Carlo simulation to obtain the crack-size distribution due to random loading is attempted, very uneconomical computation times result, and the circuit errors cannot be separated from the intended random effects of the applied loading. Finally, load-interaction effects cannot be simulated conveniently with analog equipment. Therefore, analog Monte Carlo simulation is considered to be a less useful approach to risk analysis than the estimation-theory formulation.

Regardless of the approach used for risk analysis, it has been shown that statistical treatment in terms of a damage parameter as described in Subsection 2.1, rather than directly in terms of crack size, can significantly improve the accuracy of and reduce the complexity of the analysis.

The apparent computational efficiency of estimation theory results from its avoidance of direct numerical summation of crack growth-rate equations. However, estimation theory must be formulated carefully for application to the crack-growth prediction problem, for which the dynamics are nonlinear and the statistics are non-Gaussian. Computational efficiency will depend on a formulation in terms of near-linear dynamics and near-Gaussian statistics,

which can be achieved by reformulation of the growth-rate equation in terms of a damage parameter. The growth-rate dynamics are then expanded in a Taylor series about the mean state, and the statistics of the state are approximated by the first few moments of its probability density function.

The numerical procedures for the application of estimation theory to prediction of crack-size statistics dictate that digital rather than analog computation be adopted. The resulting scheme will be able to provide the first several moments of the probability density of the damage parameter, not merely the first moment (expected value). This information can be used to estimate exceedance probabilities of critical values of the damage parameter (corresponding to critical-crack sizes), allowing much more accurate risk analysis than is possible with present schemes. The computational costs are expected to be comparable with present schemes which provide only the expected value of final crack size.

Some practical questions about load models still remain to be answered, i.e. how much flight data must be analyzed to provide a good model and what counting methods should be used? However, such questions must be answered independent of the general approach taken to the problem of predicting crack growth. One question which does affect the utility of any approach is how to treat load-interaction models. With regard to the estimation-theory approach, it has been shown that retardation can be treated efficiently, on a cycle-by-cycle basis, by incorporating existing retardation models in the flight-data-reduction scheme. Appropriately adjusted random-load statistics can then be used in an estimation-theory formulation of the prediction problem for an airplane life. Therefore, the estimation-theory approach for risk analysis of cracks propagating under random loads is promising and warrants continued development.

4.4 Recommendations

The use of a suitably defined "damage parameter", rather than crack size itself, is highly recommended for any statistical analysis of fatigue damage, regardless of the approach taken. The slight inconvenience of working with a less-than-obvious random variable is more than offset by the improved accuracy and efficiency obtained with the damage parameter. Final results may always be transformed for presentation in terms of crack size itself, if desired.

Direct inspection of large quantities of actual flight data is recommended to obtain the important statistics of loading sequences for utilization in risk analyses. Although this entails a substantial effort, the effort required to obtain such statistics when given an analytically describable approximate load model may not be significantly less. In addition, direct inspection of the flight data avoids the errors associated with analytically describable approximate models.

Further development of the application of estimation theory to aircraft fatigue damage risk analysis is recommended. The techniques of estimation theory, when applied to analysis of damage in terms of an appropriately chosen damage parameter, promise to provide efficiency and accuracy in risk analysis greater than can be obtained by present methods.

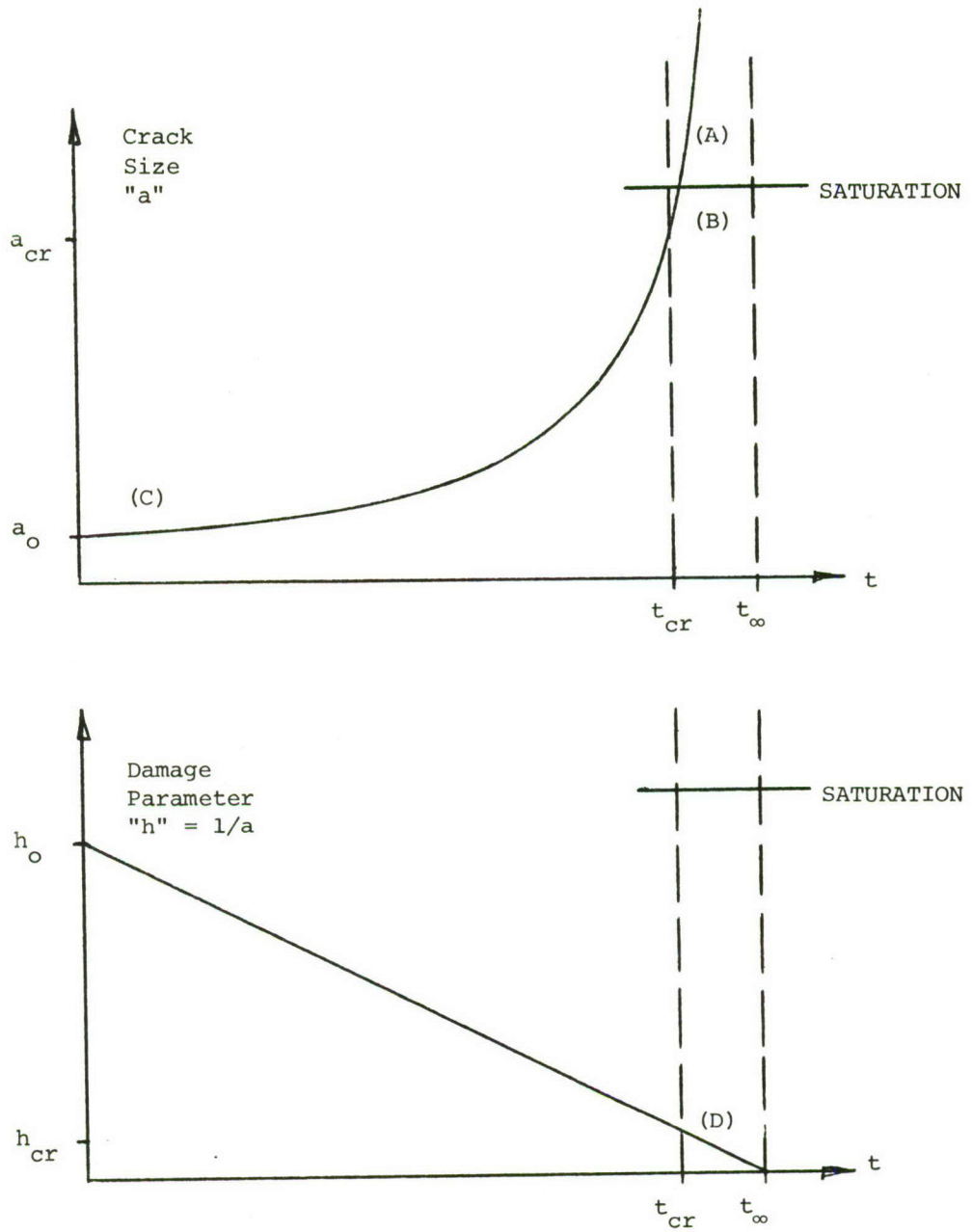


FIG. 1 COMPARISON OF TIME-HISTORIES OF CRACK SIZE AND DAMAGE PARAMETER FOR PARIS EQUATION

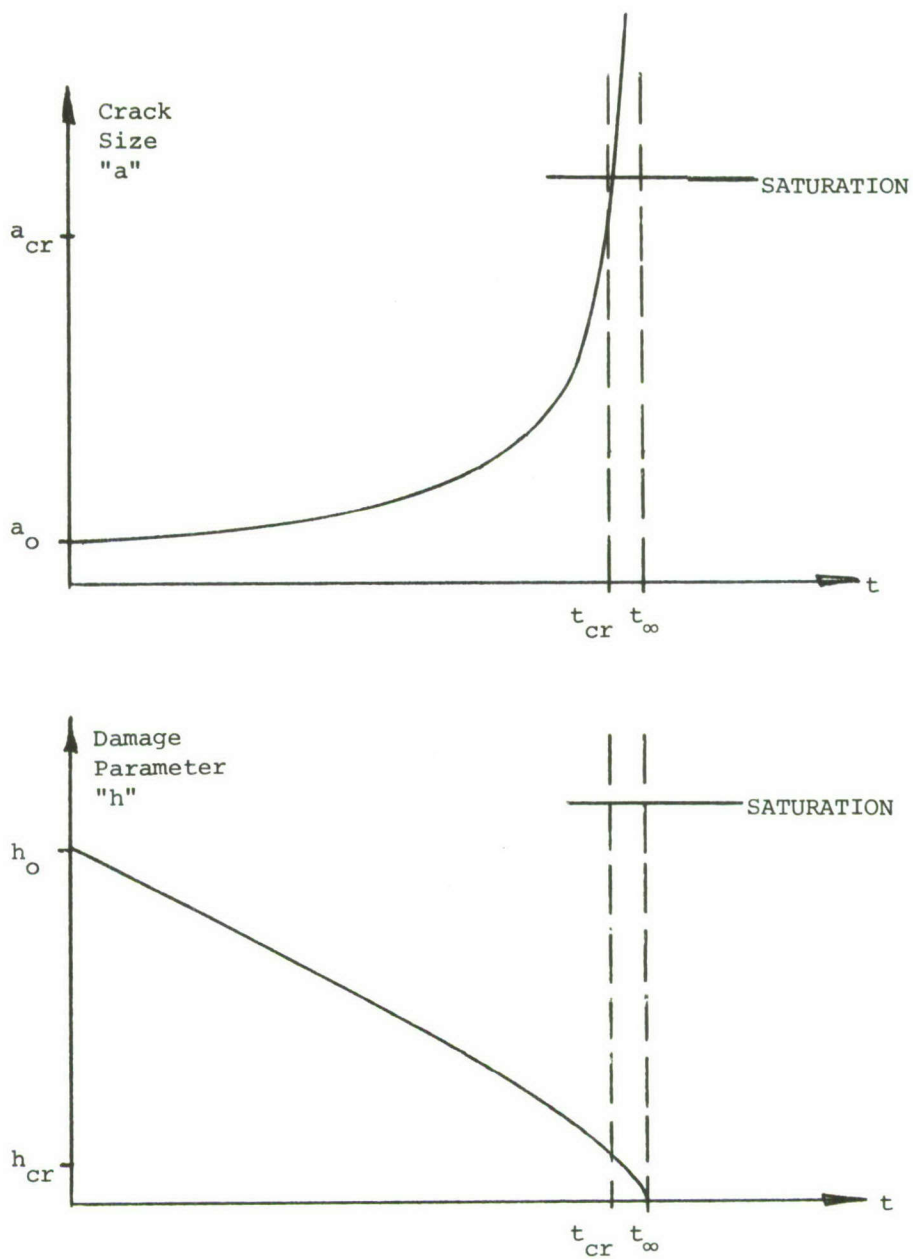


FIG. 2 COMPARISON OF TIME-HISTORIES OF CRACK SIZE AND DAMAGE PARAMETER FOR FORMAN EQUATION

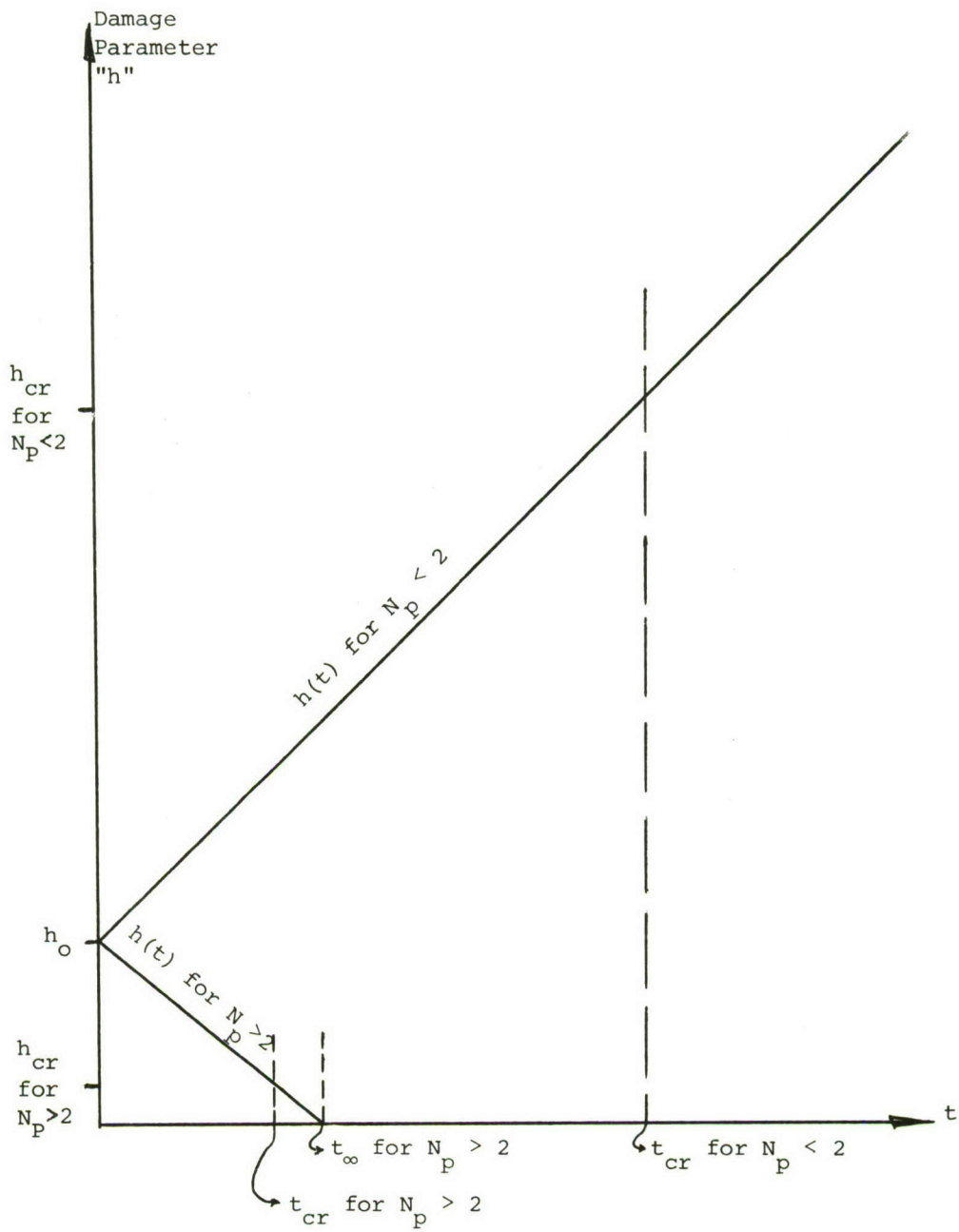


FIG. 3 COMPARISON OF TIME-HISTORIES OF DAMAGE PARAMETER FOR PARIS EQUATION, FOR $N_p > 2$ AND $N_p < 2$

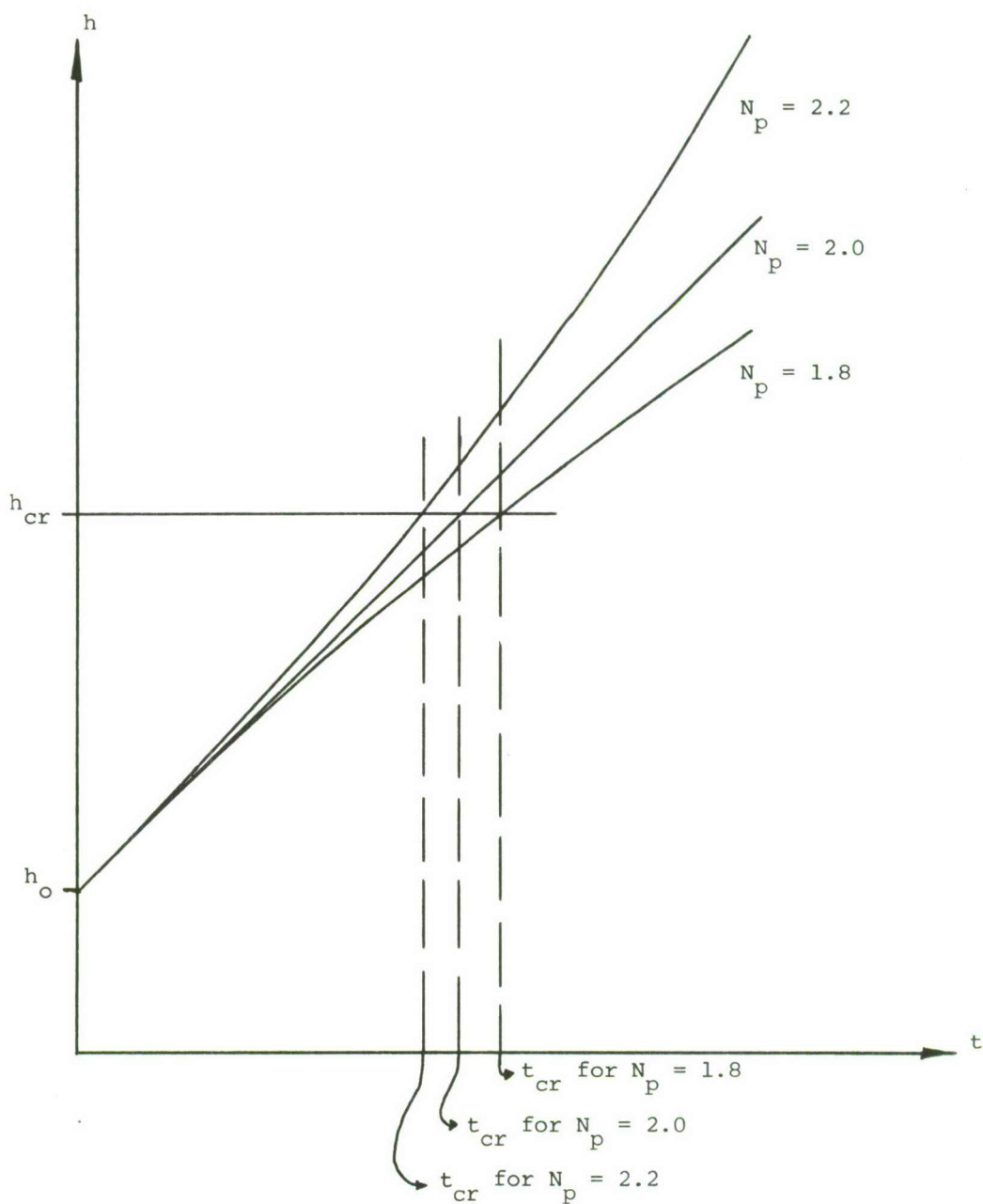


FIG. 4 COMPARISON OF TIME HISTORIES OF DAMAGE PARAMETER $h = \ln(a)$ FOR PARIS EQUATION WITH N_p NEAR TWO

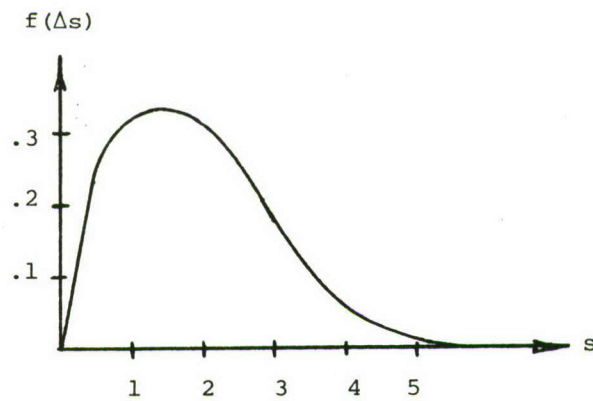
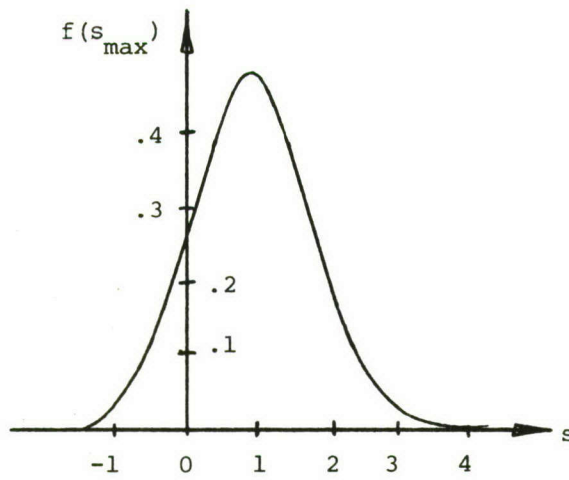


FIG. 5 PROBABILITY DENSITY FUNCTIONS FOR s_{\max} AND Δs , FOR BAND-LIMITED WHITE NOISE

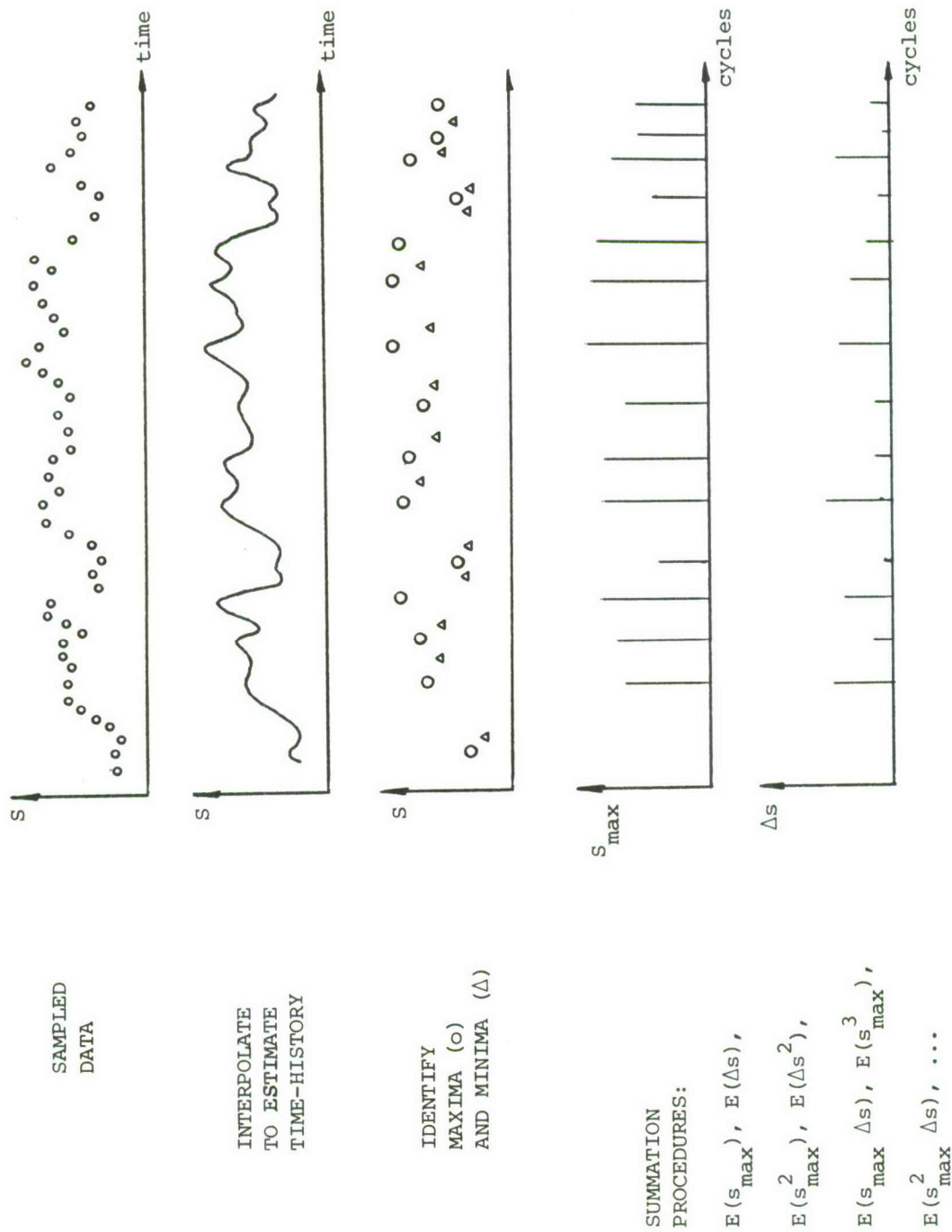
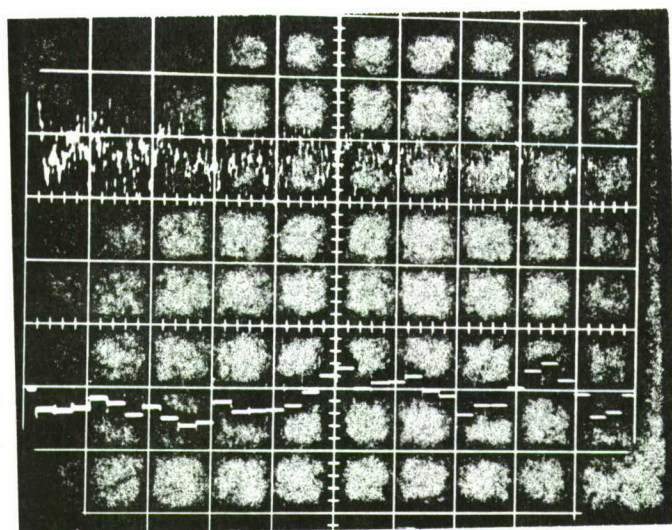
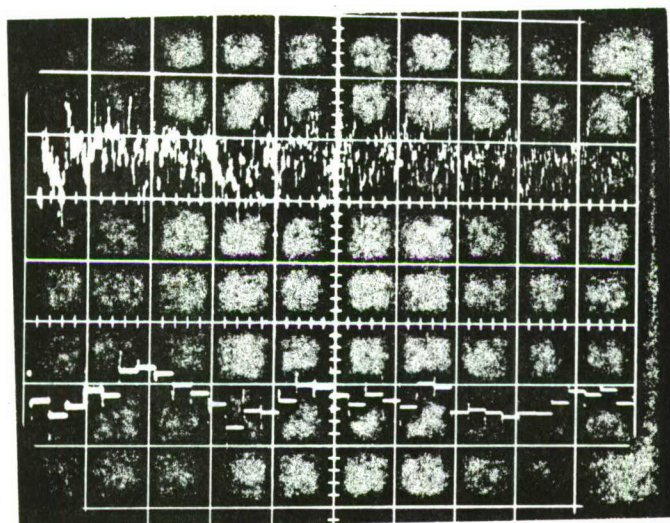


FIG. 6 REDUCTION OF SAMPLED FLIGHT DATA TO LOAD STATISTICS



NOISE
GENERATOR

SAMPLED-
AND-HELD
SIGNAL



NOISE
GENERATOR

SAMPLED-
AND-HELD
SIGNAL

Each box: Horizontally, 5 msec
Vertically, 1 volt

FIG. 7 EXAMINATION OF SAMPLE-AND-HOLD CIRCUITRY

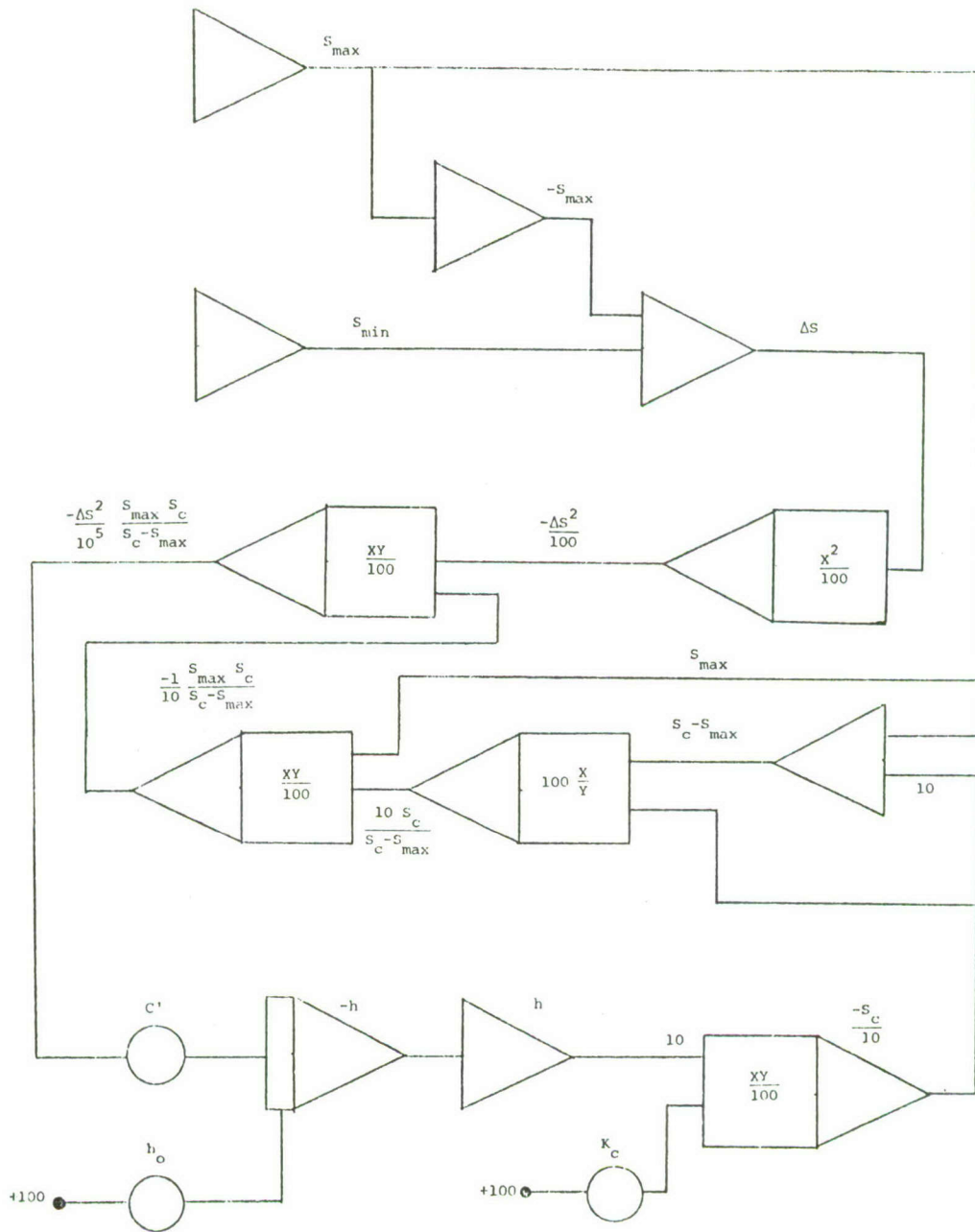
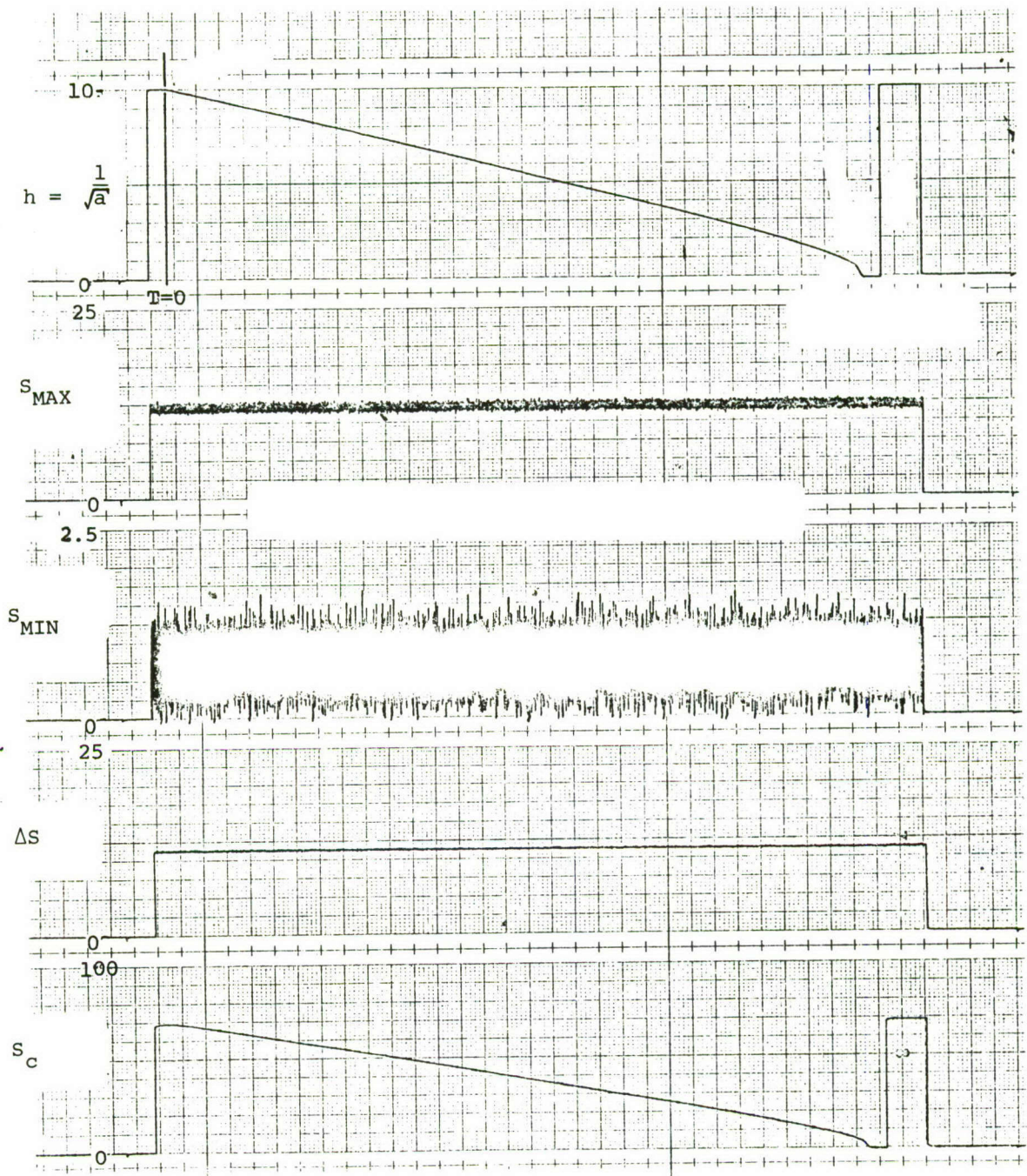


FIG. 8 FORMAN EQUATION FLOW CHART, USING DAMAGE PARAMETER "h"



s_{max} and s_{min} 1 rms white noise, $\bar{s}_{max} = 12.08$ ksi, $\bar{s}_{min} = 0.713$ ksi, $h_o = 10$

FIG. 9 ANALOG SIMULATION OF FORMAN EQUATION (REAL TIME)

s_{\max} and s_{\min} 1 rms white noise, $\bar{s}_{\max} = 20 \text{ ksi}$, $\bar{s}_{\min} = 1 \text{ ksi}$, $h_o = 10$

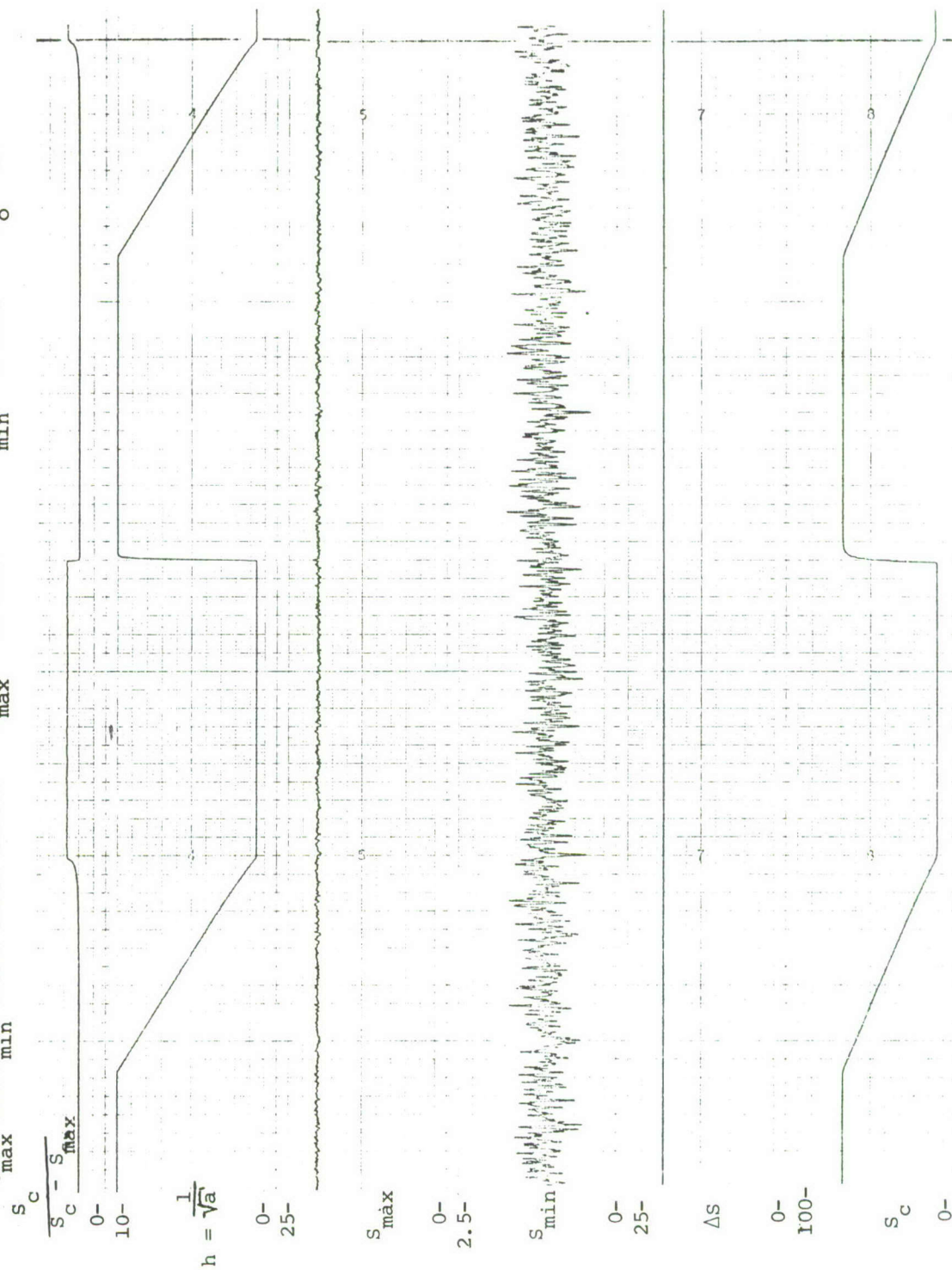


FIG. 10 ANALOG SIMULATION OF FORMAN EQUATION (REPETITIVE OPERATION)

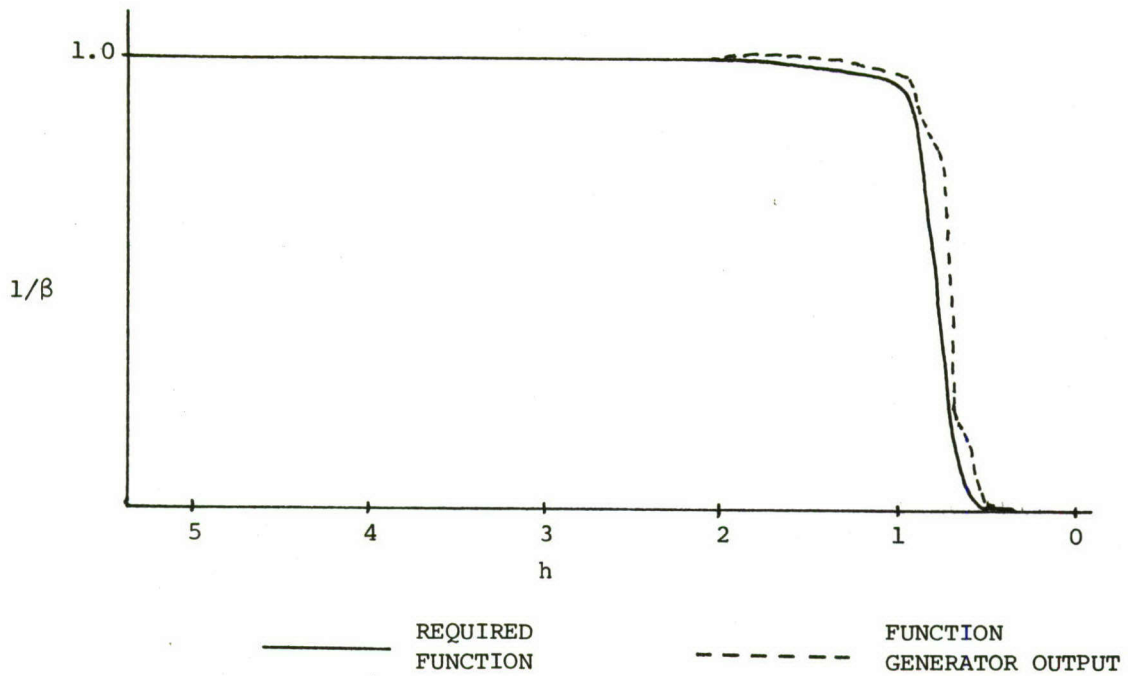


FIG. 11 FINITE PLATE CORRELATION FACTOR FOR PLATE WIDTH $b=10$ INCHES

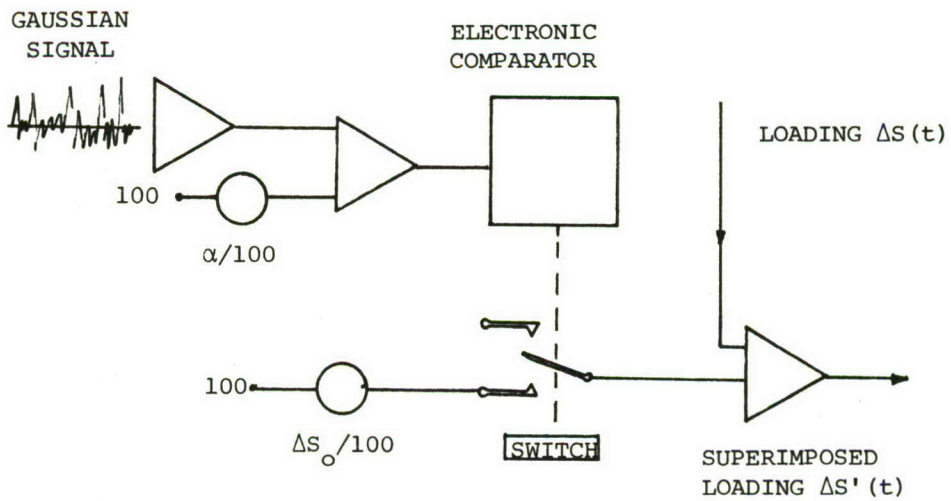


FIG. 12 ANALOG DIAGRAM FOR RANDOM APPEARANCE OF A DETERMINISTIC GAG CYCLE

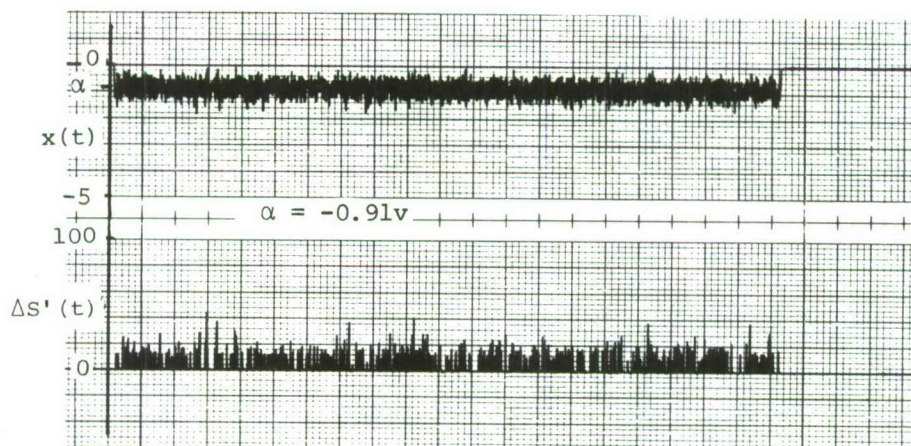
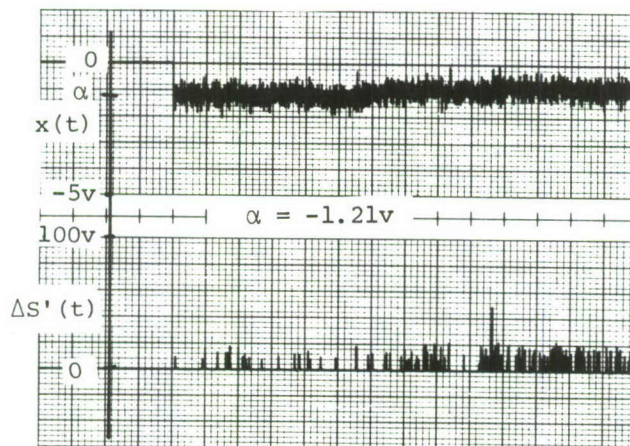
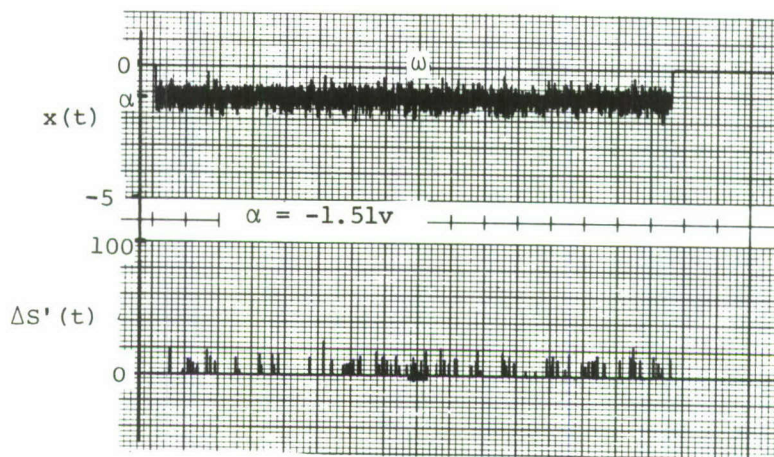


FIG. 13 EFFECT OF SWITCHING VOLTAGE BIAS ON AVERAGE TIME BETWEEN GAG CYCLES

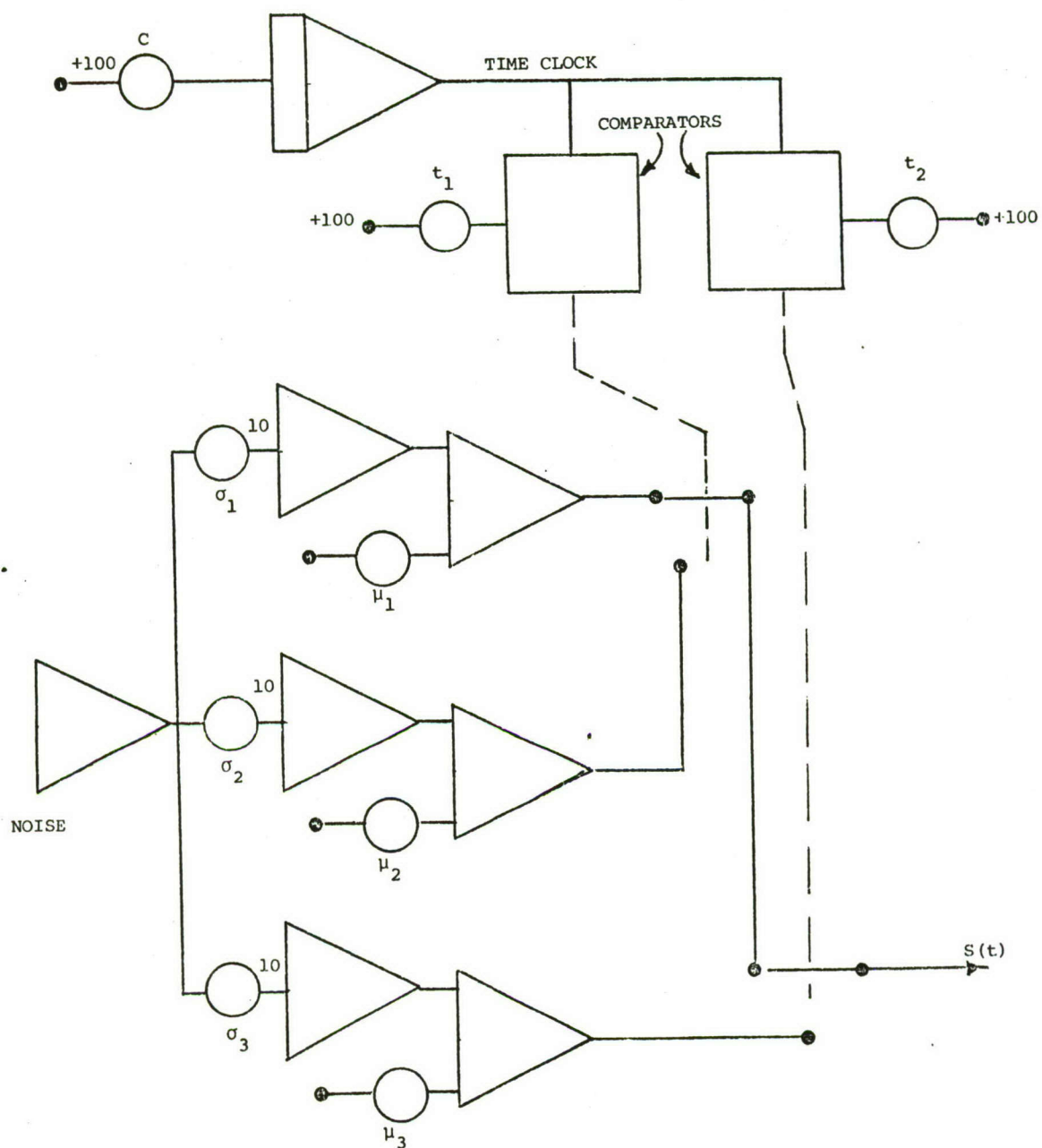
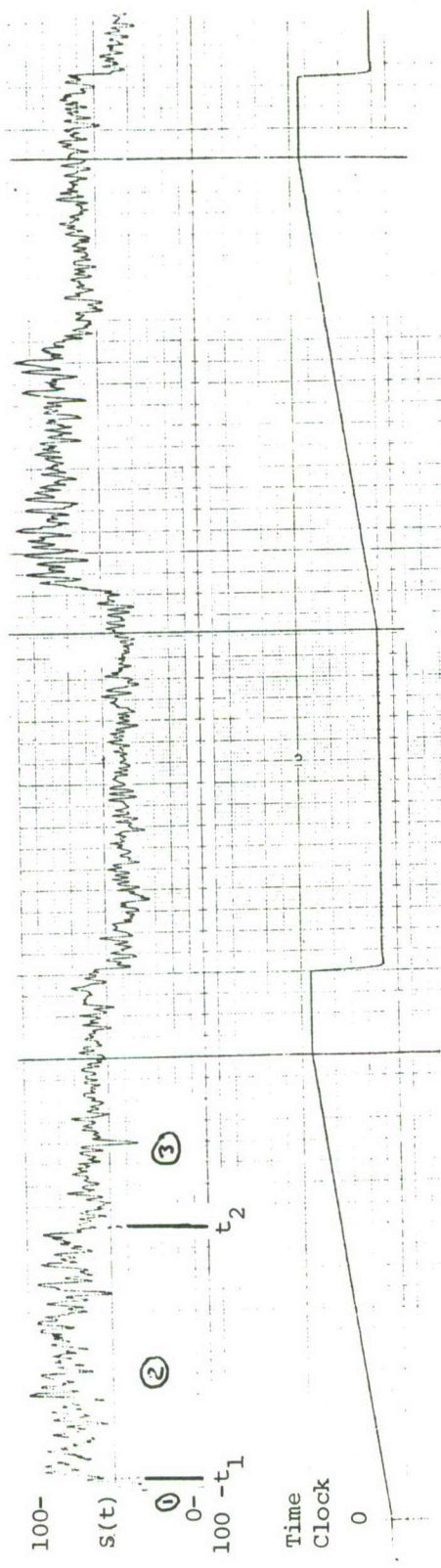


FIG. 14 ANALOG DIAGRAM FOR GAG/FLIGHT LOAD SUPERPOSITION



REGION	GAUSSIAN PARAMETERS
1	$\mu = 40 \text{ ksi}, \sigma = 10 \text{ ksi}$
2	$\mu = 80 \text{ ksi}, \sigma = 20 \text{ ksi}$
3	$\mu = 60 \text{ ksi}, \sigma = 10 \text{ ksi}$

FIG. 15 SIMULATION OF HYPOTHETICAL FLIGHT WITH THREE SEGMENTS

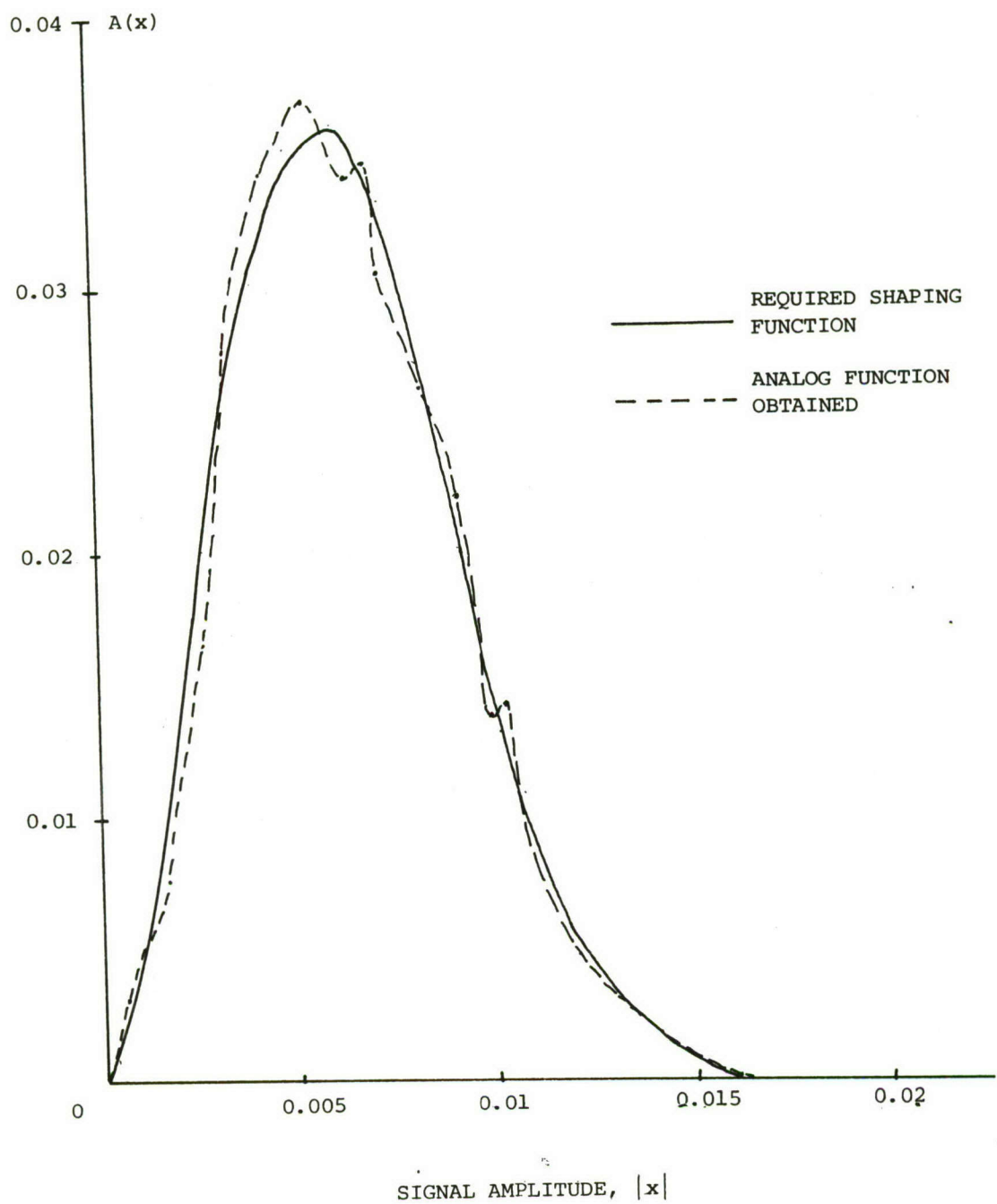


FIG. 16 GAIN FUNCTION FOR WEIBULL DISTRIBUTION SHAPING

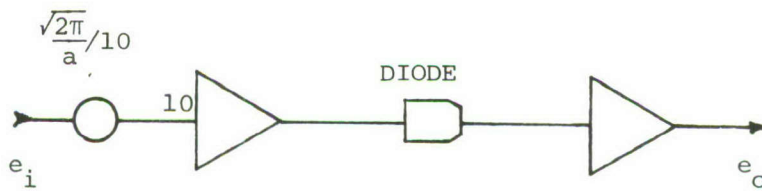
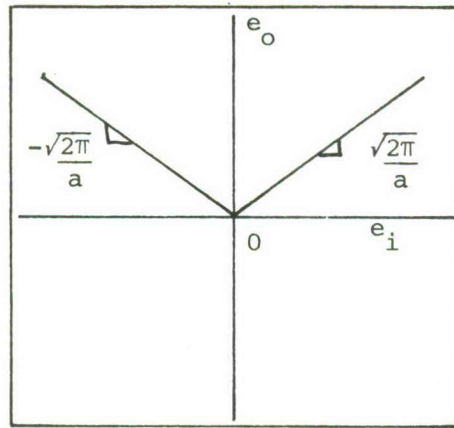


FIG. 17 SHAPING FILTER FOR RAYLEIGH NOISE

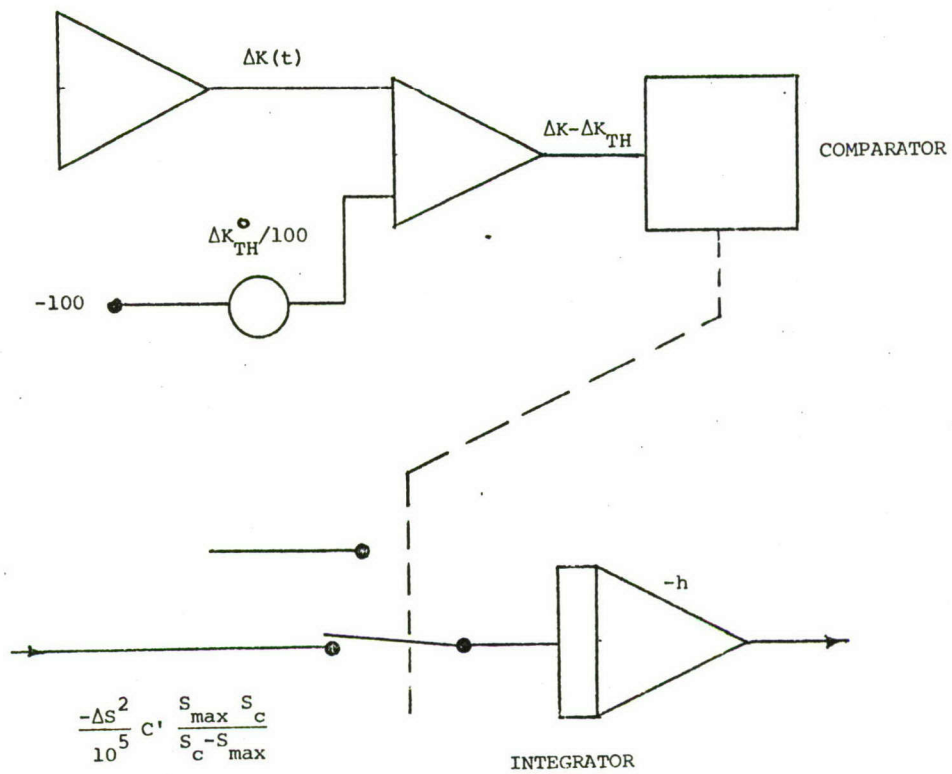
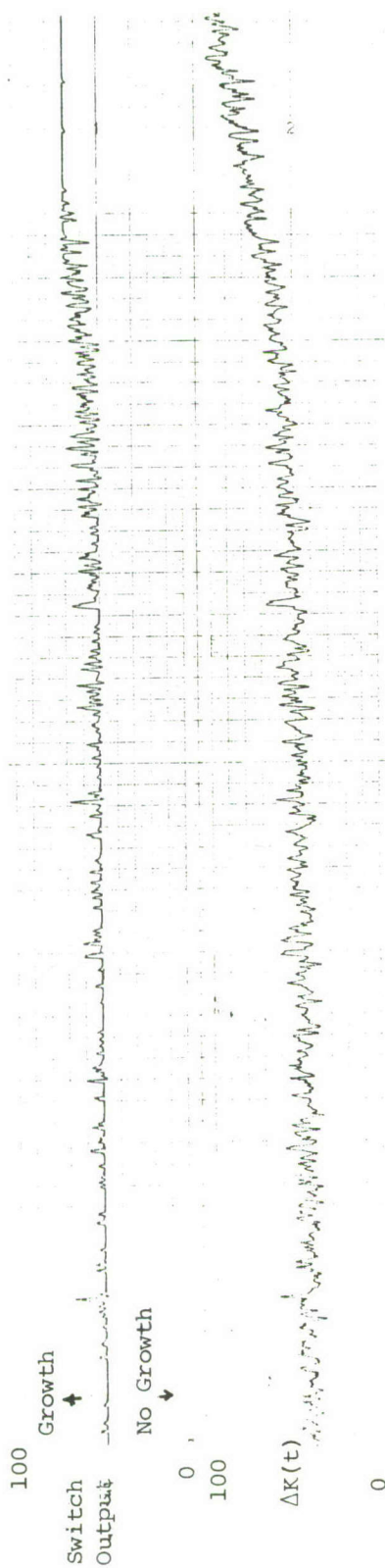


FIG. 18 STRESS INTENSITY THRESHOLD FLOW CHART



s_{\max} 1 rms white noise, $\bar{s}_{\max} = 20$ ksi

$s_{\min} = \text{constant} = 1$ ksi

$h_o = 5.75$

FIG. 19 ANALOG SIMULATION OF FORMAN EQUATION WITH STRESS INTENSITY THRESHOLD

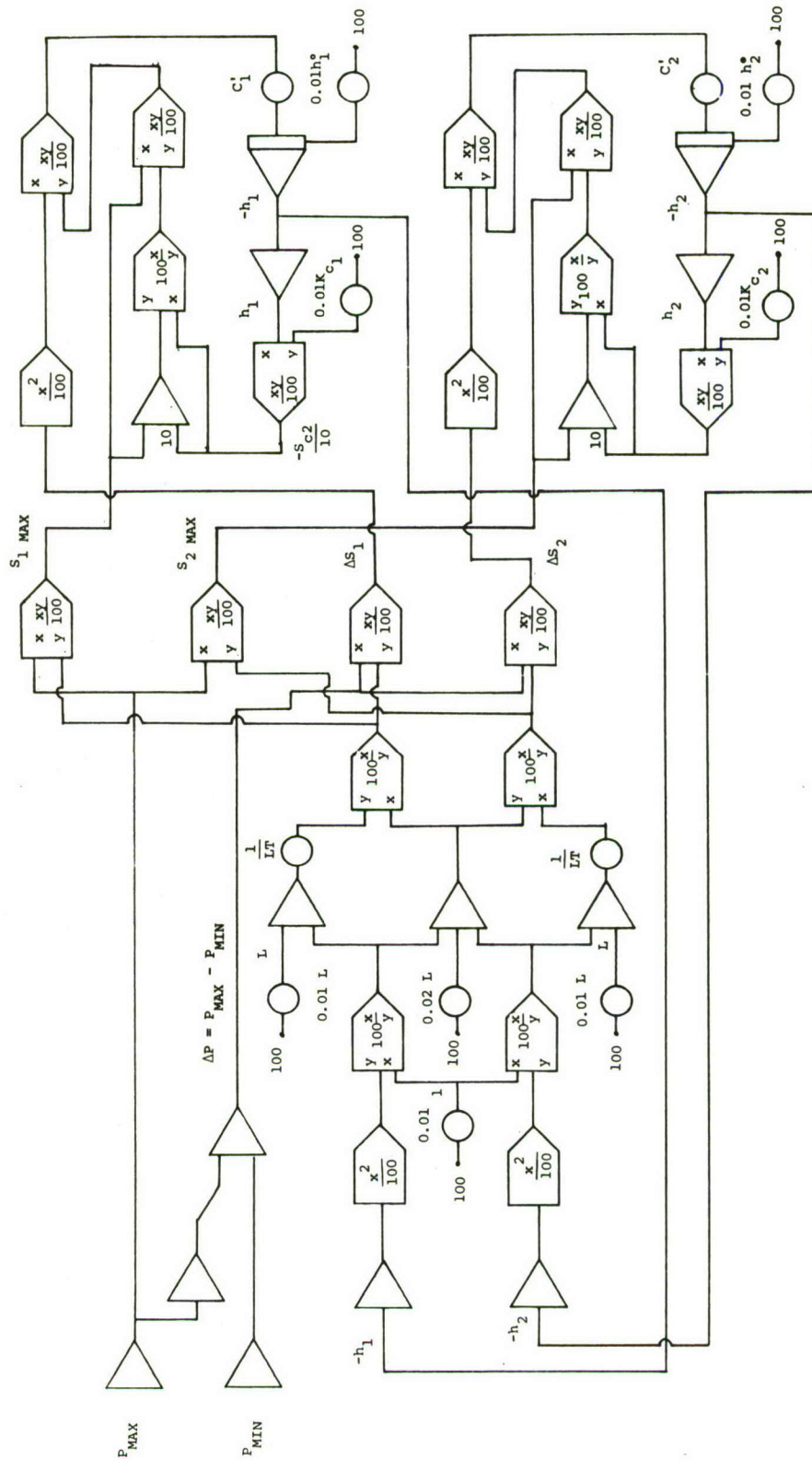


FIG. 20 FLOW CHART FOR SIMULATION OF COUPLED CRACK GROWTH

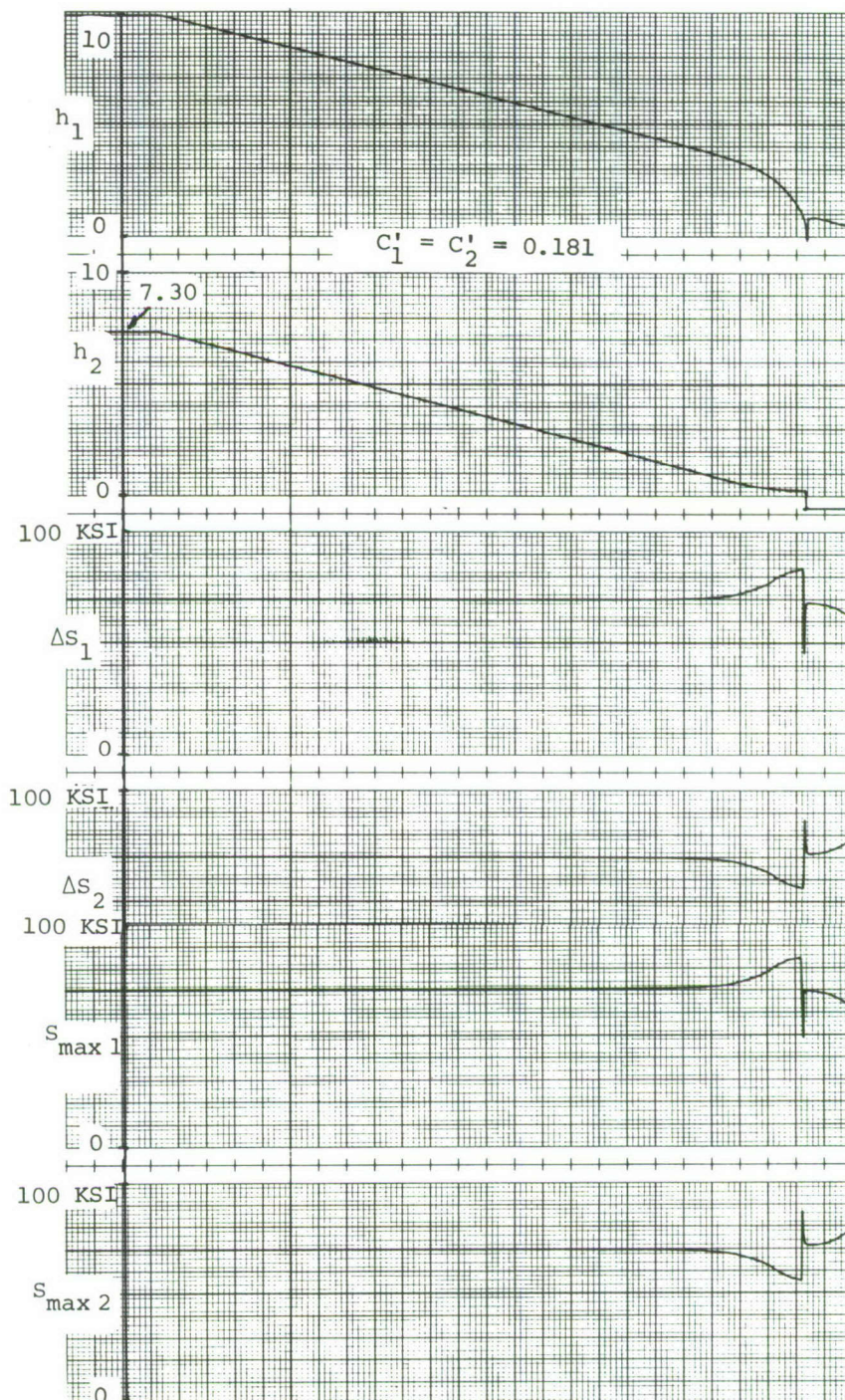


FIG. 21 ANALOG SIMULATION OF THE GROWTH OF TWO COUPLED CRACKS WITH DIFFERENT INITIAL SIZES

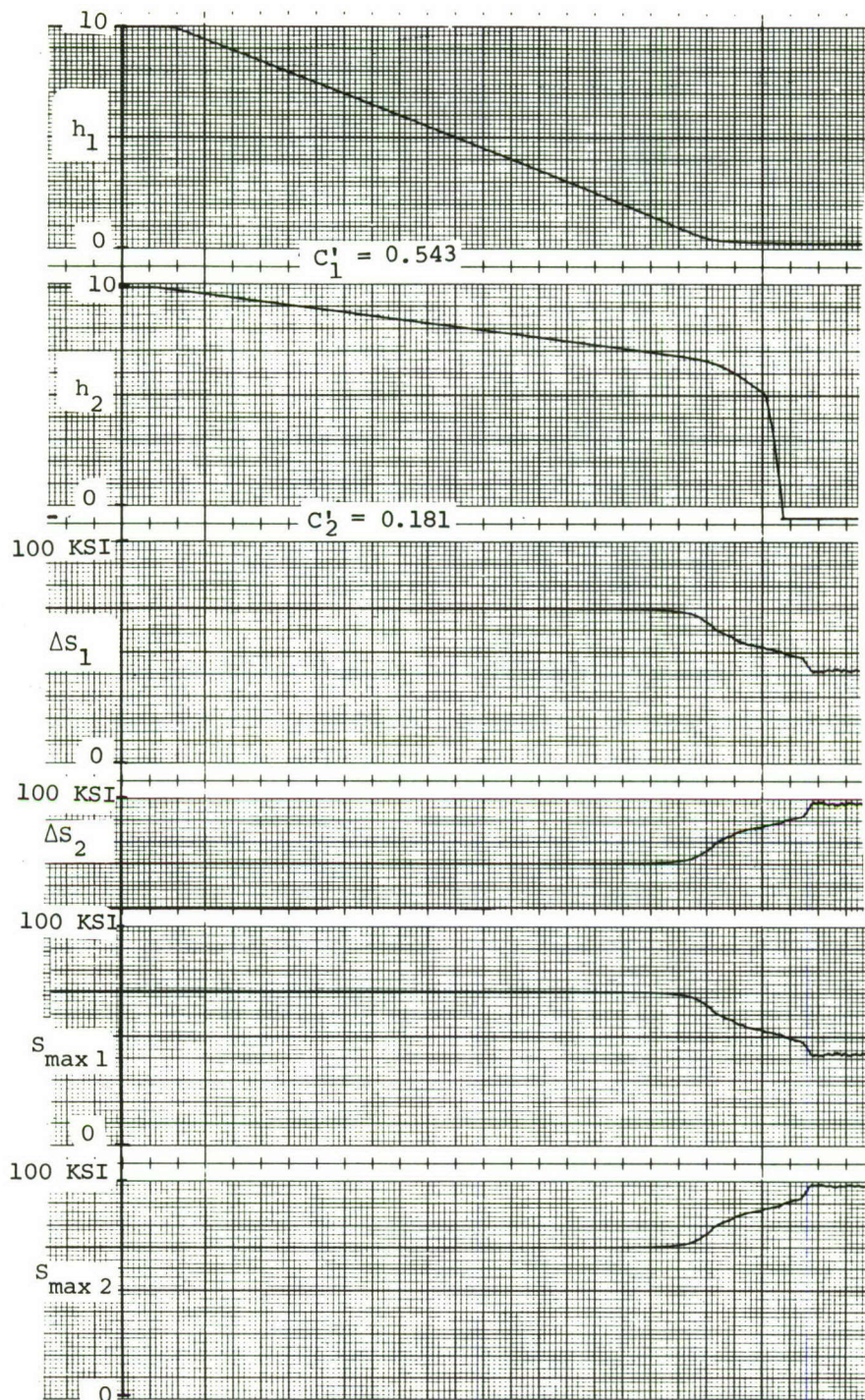


FIG. 22 ANALOG SIMULATION OF THE GROWTH OF TWO INITIALLY EQUAL COUPLED CRACKS AT DIFFERENT RATES

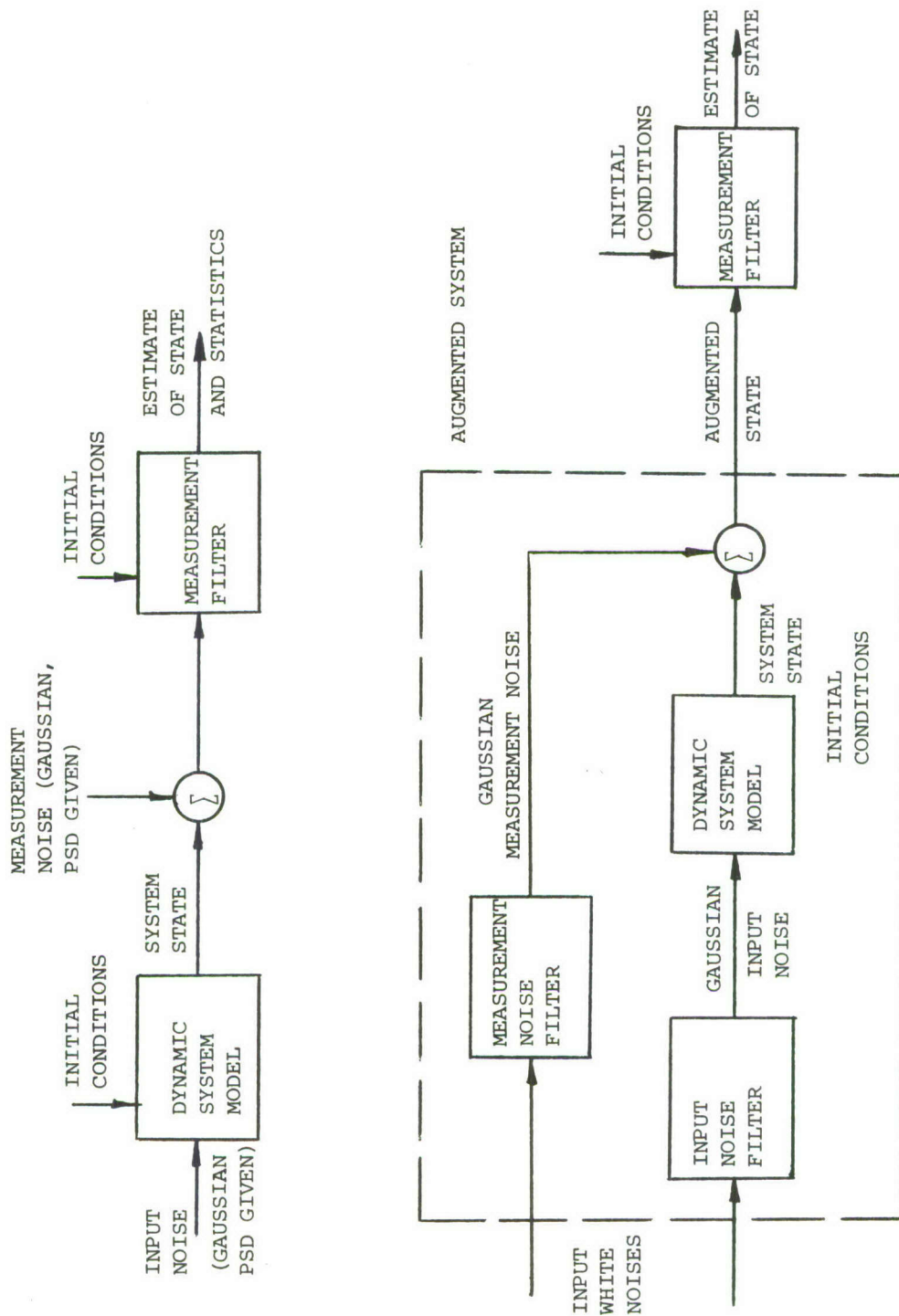
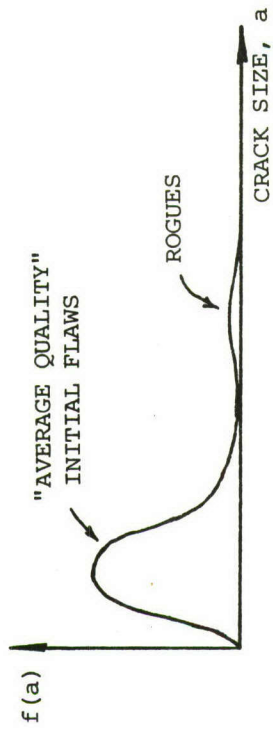


FIG. 23 SCHEMATIC DIAGRAM OF ESTIMATION THEORY

STATISTICS OF
INITIAL CRACK
SIZE DESCRIBE
NON-GAUSSIAN
INITIAL CONDITIONS



ROGUE FLAW
DISTRIBUTIONS
ARE NOT WELL
DEFINED

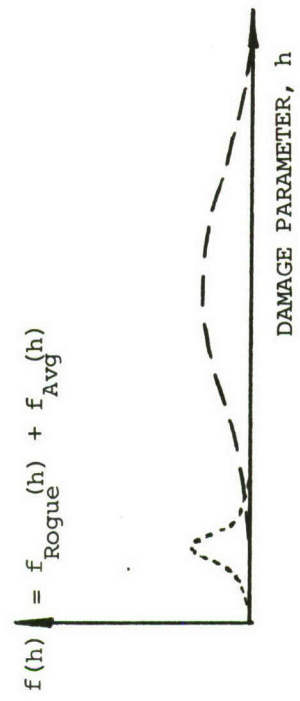
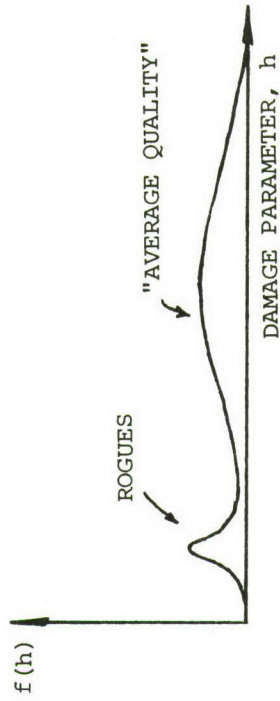


FIG. 24 TREATMENT OF BIMODAL CRACK POPULATION

APPENDIX A

FORTRAN PROGRAM FOR CALCULATION OF CRACK-GROWTH STATISTICS

```

      DIMENSION DSMU(101),DSMC(101),DS4MU(26),GMU(26),GMUE(26)
1      READ (5,901) NN,MM,MAXP
901    PCRMAT (8I10)
      IF (NN.EQ.0) STOP
2      READ (5,902) DSMEAN,DSSIGM,AZERO,CP
902    FORMAT (8F10.0)
      WRITE (6,911) NN,MM,MAXP,DSMEAN,DSSIGM,AZERO,CP
911    FORMAT ('0NN=',I5,5X,'MM=',I5,5X,'MAXP=',I5,5X,/,
1        ' DSMEAN=',F15.5,5X,'DSSIGM=',F15.5,5X,'AZERO=',
2        F15.5,5X,'CP=',F16.8)
C
C FIND DSMU, WHERE DSMU(I) = (I+1)TH CENTRAL MOMENT OF DS
C
      MAXK = MAXP * 4
      MAXKP = MAXK + 1
      MAXPP = MAXP + 1
      DSMU(1) = 1.
      DO 100 I = 2,MAXK,2
100    DSMU(I) = 0.
      DSS2 = DSSIGM**2
      DSSP = 1.
      AMULT = 1.
      DO 110 I = 3,MAXKP,2
      DSSP = DSSP*DSS2
      AMULT = AMULT * FLCAT(I-2)
110    DSMU(I) = AMULT * DSSP
      WRITE (6,913) (DSMU(I),I=1,MAXKP)
913    FORMAT (' DSMU',/,6(3X,E16.9))
C
C FIND DSMC WHERE DSMC(I) = (I+1)TH MOMENT ABOUT ZERO OF DS
C
      DSMC(1) = 1.
      FACTK = 1.
      DO 200 K = 1,MAXK
      FACTK = FACTK * FLOAT(K)
      FACTKR = FACTK
      IR = 0
      DSMC(K+1) = 0.
      FACTR = 1.
      DSMR = 1.
C ADD CONTRIBUTION FOR THIS IR
150    DSMC(K+1) = DSMC(K+1) + DSMR * DSMU(K-IR+1)
1        * FACTK / (FACTKR*FACTR)
C INCREASE IR
      IR = IR + 1
      IF (IR.GT.K) GO TO 170
C PREPARE FOR NEW IR CONTRIBUTION
      FACTR = FACTR * FLOAT(IR)
      FACTKR = FACTKR / FLOAT(K-IR+1)
      DSMR = DSMR * DSMEAN
      GO TO 150
170    CONTINUE
200    CONTINUE

```



```

      DS4MEN = DSMC(5)
      WRITE (6,914) (DSMC(I),I=1,MAXKP)
914   FORMAT (' DSMC',/,6(3X,E16.8))
C
C FIND DS4MU WHERE DS4MU(I) = (I+1)TH CENTRAL MOMENT OF (DS**4)
C
      DS4MU(1) = 1.
      FACTK = 1.
      DO 300 K = 1,MAXP
      FACTK = FACTK * FLOAT(K)
      FACTKR = FACTK
      IR = 0
      DS4MU(K+1) = 0.
      FACTP = 1.
      DS4MR = 1.
      AM1R = 1.
C ADD CONTRIBUTION FOR THIS IR
250   DS4MU(K+1) = DS4MU(K+1) + AM1R * DS4MR * DSMC(4*(K-IR)+1)
      1          * FACTK / (FACTR*FACTKR)
C INCREASE IR
      IR = IR + 1
      IF (IR.GT.K) GO TO 270
C PREPARE FOR NEW IR CONTRIBUTION
      FACTR = FACTR * FLOAT(IR)
      FACTKR = FACTKR / FLOAT(K-IR+1)
      DS4MR = DS4MR * DS4MEN
      AM1R = -AM1R
      GO TO 250
270   CONTINUE
300   CONTINUE
      WRITE (6,915) (DS4MU(I),I=1,MAXPP)
915   FORMAT (' DS4MU',/,6(3X,E16.8))
C
C FIND GMU WHERE GMU(I) = (I+1)TH CENTRAL MOMENT OF G
C
      GMEAN = DS4MEN
      GMU(1) = 1.
      DO 3000 NP = 1,MAXP
C
C GIVEN ---   NN = NUMBER OF ITEMS BEING SUMMED
C              NP = ORDER OF MOMENT OF PROBABILITY DENSITY OF
C                  SUM WHICH IS BEING COMPUTED
C              DS4MU = CENTRAL MOMENTS OF ITEMS BEING SUMMED
C
C DIMENSION NEACH .GE. (NP/2)
      DIMENSION NEACH(50)
C AM IS THE MOMENT OF THE SUM WHICH IS BEING COMPUTED
      AM = 0.
C PREPARE FACTNP
      FACTNP = 1.
      DO 1090 I = 1,NP
1090   FACTNP = FACTNP * FLCAT(I)
C

```

C PREPARE FIRST COMBINATION

C

```
K = NP/2
IF (NN.IT.K) K = NN
IF (K.EQ.0) GO TO 2000
LEVEL = 1
DO 1100 I = 1,K
1100 NEACH(I) = 2
NEACH(1) = NP - 2*(K-1)
```

C

C PREPARE FACTN AND FACTK FOR NEW K

C

```
1150 FACTN = 1.
DO 1160 I = 1,K
1160 FACTN = FACTN * FLOAT(NN+1-I)
```

C

C COMPUTE CONTRIBUTION OF THIS CONFIGURATION

C

```
1200 FACTB = 1.
FACTNB = 1.
INB = 1
DO 1220 I = 1,K
KB = NEACH(I)
IF (I.EQ.1) GO TO 1210
INB = INB + 1
IF (NEACH(I).NE.NEACH(I-1)) INB = 1
1210 FACTNB = FACTNB * FLOAT(INB)
DO 1220 J = 2,KB
1220 FACTB = FACTB * FLOAT(J)
AMP = FACTN * FACTNB / (FACTB * FACTNB)
DO 1240 I = 1,K
1240 AMP = AMP * DS4MU(NEACH(I)+1)
AM = AM + AMP
```

C

C LOOK FOR NEXT EXAMPLE

C

```
IF (K.EQ.1) GO TO 2000
LEVTRY = LEVEL + 1
IF (LEVTRY.EQ.K) LEVTRY = LEVEL
1260 IF ((NEACH(LEVTRY)-1).LE.NEACH(LEVTRY+1)) GO TO 1400
LEVEL = LEVTRY
NEACH(LEVEL) = NEACH(LEVEL) - 1
NEACH(LEVEL+1) = NEACH(LEVEL+1) + 1
GO TO 1200
```

C

C REDUCE LEVTRY

C

```
1400 LTP = LEVTRY + 1
NEXCES = 0
DO 1270 I = LTP,K
NEXCES = NEXCES + NEACH(I) - 2
1270 NEACH(I) = 2
NEACH(LEVTRY) = NEACH(LEVTRY) + NEXCES
```

```

      LEVTRY = LEVTRY - 1
      IF (LEVTRY.GE.1) GO TO 1260
C
C LEVTRY REACHED ZERO ---
C   WHICH MEANS IT IS TIME TO REDUCE K
      K = K - 1
      IF (K.EQ.0) GO TO 2000
      NEACH(1) = NEACH (1) + 2
      LEVEL = 1
      GO TO 1150
C
2000  CONTINUE
3000  GMU(NP+1) = AM / FLOAT(NN)**NP
      WRITE (6,916) (GMU(I),I=1,MAXPP)
916   FORMAT (' GMU',/,6(3X,E16.8))
C
C FIND GMUE WHICH IS THE 'ECCENTRICITIES' OF G
C   GMUE(I) = (I+1)TH ECCENTRICITY
C
      GMUE(1) = 0.
      GMUE(2) = 0.
      GMUE(3) = 0.
      AMULT = 1.
      RGMU2 = (GMU(3)**.5)
      DO 3500 K = 3,MAXP,2
      GMUE(K+1) = GMU (K+1) / (RGMU2**K)
      IF ((K+1).GT.MAXP) GO TC 3500
      AMULT = AMULT * FLOAT(K)
      GMUE(K+2) = GMU(K+2) / (RGMU2**(K+1)) - AMULT
3500  CONTINUE
      WRITE (6,917) (GMUE(I),I=1,MAXPP)
917   FORMAT (' GMUE',/,6(3X,E16.8))
      DHMEAN = -CP * MM * GMEAN
      DHMU2 = (CP*FLOAT(MM))**2 * GMU(3)
      WRITE (6,922) GMEAN,DHMEAN,DHMU2
922   FORMAT (' GMEAN=',F15.5,5X,'DHMEAN=',F15.5,5X,'DHMU2=',F15.5)
      GO TC 1
      END

```


SAMPLE OUTPUT

[illegible]

13.3K CYCLES

20K CYCLES

DSMC	0.10000000E+01	0.22500000F+02	0.53540991E+03	0.13358922E+05	0.34741331E+06	0.93749830E+07
	0.26153994E+09	0.75260150E+10	0.22273111E+12	0.67671163E+13	0.21071358E+15	0.67143336E+16
	0.21866105E+18	0.72693662E+19	0.24645099E+21	0.85127941E+22	0.29933553E+24	0.10706775E+26
	0.38923858E+27	0.14378775E+29	0.53920457E+30	0.20517792E+32	0.79183659E+33	0.30978925E+35
	0.12280951E+37					
DSMU	0.10000000E+01	0.0	0.10203516E+12	0.70384575E+17	0.11306636E+24	0.21000364E+30
	0.50256602E+36					
GMU	0.10000000E+01	0.0	0.68023378E+10	0.31282018E+15	0.16306236E+21	0.24008714E+26
	0.85845968E+31					
GMUP	0.0	0.0	0.0	0.55757993E+00	0.52400780E+00	0.62910461E+01
	0.12273727E+02					
GMZAN=	347413.312	DMEAN=	-18.06653	DHMU2=	18.39563	
NN=	22	NN=	20000	NXP=	6	
DSMEAN=	22.50000	DSSIGN=				
DSMU	0.10000000E+01	0.0	0.29159988E+02	0.0	0.25509141E+04	0.0
	0.37192306E+06	0.0	0.75916896E+08	0.0	0.19923624E+11	0.0
	0.63906974E+13	0.0	0.24225844E+16	0.0	0.10596379E+19	0.0
	0.52528325E+21	0.0	0.29102780E+24	0.0	0.17821366E+27	0.0
	0.11952423E+30					
DSMO	0.10000000E+01	0.22500000E+02	0.53540991E+03	0.13358922E+05	0.34741331E+06	0.93749830E+07
	0.26153994E+09	0.75260150E+10	0.22273111E+12	0.67671163E+13	0.21071358E+15	0.67143336E+16
	0.21866105E+18	0.72693662E+19	0.24645099E+21	0.85127941E+22	0.29933553E+24	0.10706775E+26
	0.38923858E+27	0.14378775E+29	0.53920457E+30	0.20517792E+32	0.79183659E+33	0.30978925E+35
	0.12280951E+37					
DSUP	0.10000000E+01	0.0	0.10203516E+12	0.70384575E+17	0.11306636E+24	0.21000364E+30
	0.50256602E+36					
GMU	0.10000000E+01	0.0	0.68023378E+10	0.31282018E+15	0.16306236E+21	0.24008714E+26
	0.85845968E+31					
GMUP	0.0	0.0	0.0	0.55757993E+00	0.52400780E+00	0.62910461E+01
	0.12273727E+02					
GMZAN=	347413.312	DMEAN=	-27.16771	DHMU2=	28.36220	
CP=	0.39099994E-03					

APPENDIX C
COMMERCIAL HYBRID COMPUTER MANUFACTURERS

MANUFACTURER	COMMENT
ADAGE, INC. 1079 Commonwealth Ave. Brighton, Mass. 02159	Mostly Display Equipment
APPLIED DYNAMICS COMPUTER SYSTEMS 2275 Pratt Road Ann Arbor, Mich. 40104	DELTA FOUR Plug & Logic to IBM/360 & XDS/SIGMA Optimization & Simulation
COMDYNA INC. N.A.	Model 648 Plug & Logic to EAI Simulation & Student Training
ELECTRONIC ASSOCIATES, INC. (EAI)* 185 Normouth Parkway West Long Branch, N.J. 07764	590, 690, 7945 Simulation
GPS INSTRUMENT COMPANY, INC. 188 Needham Street Newton, Mass. 02164	200T System
SYSTRON-DONNER CONCORD INSTRUMENT DIVISION* 888 Galindo Street Concord, California 94520	Model 80Y Simulation & On-Line Control

* Manufacturers which responded to survey.

APPENDIX D
HYBRID COMPUTER FEATURES

Item	EAI Pacer 500-700 Series ⁽¹⁾	Systron-Donner System 80 H ⁽¹⁾	Wright-Patterson Astrodata Hybrid with CI-5000/5 Analog
Integration/Summation Units	8-42	10-24	85
Summation Units	8-54	36-112 ⁽²⁾	85
Multiplier Units	2-60	4-114	171 ⁽³⁾
Single Variable Function Generators	0-36	3-15	37
Comparators/ Switching Units	2-36	9-24	56
Analog Multi-Variable Function Generators Available	Yes ⁽⁴⁾	No	No
Digital Core	8K-32K	?	Maximum Unknown
Comments	Wide variety of peripherals and accessories available	Includes UNIBUS PDP-11 central processor	

- (1) Numbers dependent upon specific model and/or series selected. Range of values given.
- (2) Number of operational amplifiers given. May be used as integrators or summers.
- (3) Includes inverters and resolvers.
- (4) Some computation performed digitally.

REFERENCES

1. Military Specification, "Airplane Damage Tolerance Requirements", MIL-A-83444 (USAF), 2 July 1974.
2. Wood, H.A., "Application of Fracture Mechanics to Aircraft Structural Integrity", J Eng Fract Mech, Vol. 432, 1975, pp. 1-8.
3. Holpp, J.E. and Landy, M.A., "The Development of Fatigue/Crack Growth Analysis Loading Spectra", NATO Advisory Group for Aerospace Research and Development, AGARD-R-640, January 1976.
4. Shinozuka, M., "Development of Reliability-Based Aircraft Safety Criteria: An Impact Analysis", Modern Analysis, Inc., Ridgewood, NJ, AFFDL-TR-76-36, April 1976.
5. Reeves, P.M., Joppa, R.G. and Ganzer, V.M., "A Non-Gaussian Model of Continuous Atmospheric Turbulence Proposed for Use in Aircraft Design", AIAA Paper 75-31, 1975.
6. Anon., "Structural Review, F-4C/D/E ASIP, Volume I", McDonnell-Douglas Corp., St. Louis, MO, 26-27 April 1974.
7. Paris, P.C., "The Fracture Mechanics Approach to Fatigue", Fatigue: An Interdisciplinary Approach (J.J. Burke, N.L. Reed and V. Weiss, ed.), Syracuse University Press, 1964, pp. 107-132.
8. Palmgren, A., "Die Lebensdauer von Kugellager", ZVDI, Vol. 68, 1924, pp. 339-341.
9. Miner, M.A., "Cumulative Damage in Fatigue", J Appl Mech, Vol. 12, 1945 pp. A159-A164.
10. Forman, R.G., Kearney, V.E. and Engle, R.M., "Numerical Analysis of Crack Propagation in Cyclically Loaded Structures", Trans ASME, Series D, J Basic Eng, Vol. 89, September 1967, pp. 459-464.
11. Burris, P.M. and Bender, M.A., "Aircraft Load Alleviation and Mode Stabilization (LAMS)", The Boeing Company and Honeywell, Inc., AFFDL-TR-68-148, April 1969.
12. Orringer, O., Ehrenbeck, R. and Tong, P., "Development of Design and Test Criteria for the Structural Integrity of Rail Vehicle Mechanical Systems", Case Studies in Fracture Mechanics (T.P. Rich and D.J. Cartwright, ed.), U.S. Army Materials and Mechanics Research Center, Watertown, MA, to appear in 1977.

13. Schjive, J., "The Accumulation of Fatigue Damage in Aircraft Materials and Structures", NATO Advisory Group for Aerospace Research and Development, AGARD-AG-157, January 1972.
14. Wheeler, O.E., "Crack Propagation Under Spectrum Loading", General Dynamics, Fort Worth Div., Report No. FZM-5602, June 1970.
15. Willenborg, J.D., Engle, R.M. and Wood, H.A., "A Crack Growth Retardation Model Using an Effective Stress Concept", U.S. Air Force Flight Dynamics Laboratory (AFFDL/FBE), Wright-Patterson Air Force Base, Ohio, AFFDL-TM-FBR-71-1, January 1971.
16. Dill, H.D. and Saff, C.R., "Spectrum Crack Growth Prediction Method Based on Crack Surface Displacement and Contact Analyses", Fatigue Crack Growth Under Spectrum Loads, American Society for Testing and Materials, ASTM STP 595, 1976, pp. 306-319.
17. Engle, R.M., "CRACKS, A Fortran IV Digital Computer Program for Crack Propagation Analysis", U.S. Air Force Flight Dynamics Laboratory (AFFDL/FBE), Wright-Patterson AFB, Ohio, AFFDL-TR-70-107, October 1970.
18. Gallagher, J.P., "Estimating Fatigue=Crack Lives for Aircraft: Techniques", J Exp Mech, Vol. 16, No. 11, November 1976, pp. 425-433.
19. Orringer, O., Harris, R.F. and McCarthy, J.F., "Analog Computation Assessment of the Risk of Structural Failure Due to Crack Growth Under Random Loading", Aeroelastic and Structures Research Laboratory, MIT, Cambridge, MA, AFFDL-TR-75-123, October 1975.
20. Campbell, J.E. et al., Damage Tolerant Design Handbook, Metals and Ceramics Information Center, Battelle-Columbus Laboratories, Columbus, Ohio, MCIC-HB-01, 1973.
21. Jazwinski, A.H., Stochastic Processes and Filtering Theory, Academic Press, New York, 1970.
22. Sage, A.P. and Melsa, J.L., Estimation Theory with Applications to Communications and Control, McGraw-Hill, New York, 1971.
23. Clough, R.W. and Penzien, J., Dynamics of Structures, McGraw-Hill, New York, 1975.
24. Rice, J.R., "Theoretical Prediction of Some Statistical Characteristics of Random Loadings Relevant to Fatigue and Fracture", PhD Thesis, Department of Engineering Mechanics, Lehigh University, Bethlehem, PA, 1964.

25. Rice, J.R. and Beer, F.P., "On the Prediction of Some Random Loading Characteristics Relevant to Fatigue", Proc. Second International Conf. on Acoustical Fatigue in Aerospace Structures, Dayton, OH, 19 April - 1 May 1964.
26. Rice, J.R. and Beer, F.P., "On the Distribution of Rises and Falls in a Continuous Random Process", J Basic Eng, ASME, 1965, pp. 398-404.
27. Hyland, D.C., "A Method for the Analysis of Nonlinear Systems Excited by Random Noise", PhD Thesis, Department of Aeronautics and Astronautics, MIT, Cambridge, MA, 1974.
28. Gnedenko, B.V., The Theory of Probability, Chelsea Publishing Co., New York, 1965.
29. Bowie, O.L., "Analysis of an Infinite Plate Containing Radial Cracks Originating at the Boundaries of an Internal Circular Hole", J Math Phys, Vol. 35 (1956), p. 60.
30. Tada, H., Paris, P.C. and Irwin, G.R., The Stress Analysis of Cracks Handbook, DEL Research Corporation, Hellertown, PA, 1973.
31. Pian, T.H.H., Orringer, O., Stalk, G. and Mar, J.W., "Numerical Computation of Stress Intensity Factors for Aircraft Structural Details by the Finite Element Method", Aeroelastic and Structures Research Laboratory, MIT, Cambridge, MA, AFFDL-TR-76-12, May 1976.
32. Bendat, J.S., Principles and Applications of Random Noise Theory, Wiley, New York, 1958.
33. Hahn, G.J. and Shapiro, S.S., Statistical Models in Engineering, Wiley, New York, 1967.